NeuroRegulation

ISNR INTERNATIONAL SOCIETY FOR NEUROREGULATION & RESEARCH

Decoding Self-Regulation in Substance Use Disorders: Machine Learning and LORETA Neurofeedback at Precuneus

Rex L. Cannon[*]

Currents, Knoxville, Tennessee, USA

Abstract

Substance use disorders (SUD) remain among the most treatment-resistant conditions, particularly in incarcerated populations. Despite decades of neuropsychological models, few approaches capture the dynamic, network-level self-regulation deficits observed in SUD. In this study, 63 incarcerated individuals completed 20 sessions of LORETA neurofeedback targeting alpha (8–13 Hz) at the left precuneus. Pre–post EEG current source density (CSD) and Personality Assessment Inventory (PAI) scores were analyzed. A Random Forest classifier was trained on spectral CSD features and behavioral deltas, with Shapley Additive Explanation (SHAP) values used to interpret model contributions. Results showed significant alpha increases at the trained ROI, accompanied by posterior-to-frontal energy redistribution and functional asymmetry. Notably, both alpha synchronization and desynchronization predicted behavioral improvement, with an overall PAI effect size of d = 0.85. Regression and PCA confirmed directional reorganization and subgroup differentiation. Cohen's d analysis revealed frequency-specific effects in alpha and low beta bands. Machine learning (ML) revealed that changes in posterior and frontal regions of interest (ROI) were differentially predictive of treatment response, and Reliable Change Index (RCI) identified responders with physiological and behavioral concordance. These findings challenge static trait-based models of addiction and suggest that rhythmic neurofeedback and ML interpretation can uncover emergent regulatory subtypes. This work proposes a shift from amplitude-based training to network-informed modulation as a foundation for scalable, individualized SUD interventions.

Keywords: EEG; neurofeedback; machine learning; artificial intelligence; learning; substance use disorders

Citation: Cannon, R. L. (2026). Decoding self-regulation in substance use disorders: Machine learning and LORETA neurofeedback at precuneus. *NeuroRegulation, 13*(1), 91–116. https://doi.org/10.15540/nr.13.1.91

***Address correspondence to**: Rex L. Cannon, PhD, BCN, Currents, LLC, 214 South Peters Rd., Ste 102, Knoxville, TN 37923, USA. Email: rcannonphd@gmail.com

Edited by:
Randall Lyle, PhD, Mount Mercy University, Cedar Rapids, Iowa, USA

Reviewed by:
John Davis, PhD, McMaster University, Hamilton, Ontario, Canada
Tanya Morosoli, MSc: 1) Clínica de Neuropsicología Diagnóstica y Terapéutica, Mexico City, Mexico; 2) PPCR, ECPE, Harvard T. H. Chan School of Public Health, Boston, Massachusetts, USA

Introduction

Substance use disorder (SUD) continues to represent one of the most costly and treatment-resistant conditions in public health, particularly in incarcerated populations (Belenko & Peugh, 2005; Mumola & Karberg, 2006). Despite decades of clinical observation, pseudostandardized treatment protocols, and policy reform, the majority of justice-involved individuals, as well as general populations in treatment settings for SUD experience high relapse rates and recidivism (Mericle et al., 2010). These outcomes suggest that our models of addiction, and especially our attempts to intervene, may be built on fundamentally incomplete understanding of brain function.

The prevailing neuropsychological models of addiction rely heavily on correlational designs, linear assumptions, and aggregate behavioral markers. Cognitive and affective dysfunctions are described primarily as trait-based deficits, to be managed or compensated for through pharmacology or behavioral methods. In more recent years, trauma

has been posited as a causative agent of addictive behaviors. Yet these models often fail to account for the dynamism of the human brain as a self-organizing system (Friston, 2010), and they offer little explanatory power for the variability observed in real-world treatment outcomes. The problem is not merely one of statistical power or sample size; it is a conceptual failure to understand the brain as a dynamic, temporally structured, and context-responsive network. In this paper, we propose a fundamentally different approach, one that integrates EEG-based current source density (CSD), machine learning (ML), and nonlinear dynamics, to uncover a replicable neurophenotype of self-regulation in incarcerated individuals with SUD.

The historical dominance of null hypothesis significance testing (NHST) in psychology and neuroscience has inadvertently constrained discovery. Most clinical studies have been bound by the $p < .05$ rule, which restricts interpretation to predefined relationships and excludes high-dimensional interactions between brain regions, frequency bands, and learning mechanisms (Cannon, 2009; Gigerenzer, 2004). This has created an illusion of empirical rigor while simultaneously filtering out critical insights that emerge from nonlinear, network-level behavior (Bassett & Sporns, 2017). As a result, the past 50 years of neuroscience research has produced thousands of "confirmed" findings, but little in the way of real predictive power for who will benefit from which interventions—or why. Although, the data in this paper has met the typical $p < .05$ rule in pre and post neurophysiological, psychometric and regression matrices, as well as rearrest rates (Cannon et al., 2025), questions remain regarding how this translates to self-regulating networks and interactions between frequencies, regions of interest (ROI) and behavioral states. ML and artificial intelligence (AI) may be methods to discover these unknowns and inspire new directions of study.

Electroencephalographic rhythms reflect more than background activity; they are intrinsic signals of regulatory processing in the central nervous system. Among these, theta (4–8 Hz) and alpha (8–13 Hz) oscillations have long been linked to core learning and self-regulatory functions (Başar et al., 2001; Klimesch, 1999). Theta is widely understood to support encoding, working memory, and attentional engagement, particularly during task-related learning and motivational conflict (Cavanagh & Frank, 2014; Mitchell et al., 2008). Meanwhile, alpha oscillations regulate cortical inhibition, sensory gating, and the timing of attentional shifts, acting as a control signal for prioritizing information streams (Jensen & Mazaheri, 2010).

Importantly, these rhythms are not confined to task states. In both resting-state and default mode network (DMN) configurations, alpha and theta jointly coordinate internally-focused processing, including emotional regulation, autobiographical memory, and self-referential thought (Knyazev, 2013; Scheeringa et al., 2008). Alterations in either rhythm have been observed across a range of psychiatric conditions, including depression, anxiety, attention-deficit/hyperactivity disorder (ADHD), and SUD (Bazanova & Vernon, 2014). In particular, disrupted theta–alpha interactions may indicate a failure to integrate affective and cognitive control mechanisms, leaving individuals vulnerable to impulsive decision-making, poor error monitoring, and dysregulated emotion.

Asymmetries in alpha and theta power across hemispheres further suggest specialized vulnerabilities in affective and regulatory processing. Left frontal regions, particularly in the alpha band, have been repeatedly implicated in the neural basis of mood, motivation, and self-directed action. Reduced alpha power in the left hemisphere (reflecting increased cortical activation) is commonly associated with approach-related tendencies, impulsivity, and risk-taking behaviors, whereas increased left alpha (relative hypoactivity) has been linked to depression, anhedonia, and withdrawal (Coan & Allen, 2004; Davidson, 2004). These asymmetries may converge with SUD pathways through mechanisms shaped by trauma, affective blunting, social disconnection, or disrupted neurodevelopment. Of particular concern is the potential compounding effect of prenatal drug exposure (PDE), which may alter the establishment of these frontal-limbic asymmetries early in life, setting the stage for later difficulties in mood regulation, attentional shifting, and behavioral inhibition. Future studies should directly examine whether alpha and theta asymmetry patterns in PDE-affected children parallel those found in SUD populations, offering a possible early biomarker of self-regulatory vulnerability (Koponen, et al., 2020).

Together, these rhythmic patterns participate in the oscillatory infrastructure of self-regulation. Our approach to neurofeedback and its ML-based analysis, is grounded in the idea that meaningful change must occur within these rhythms, not apart

from them. They are not background noise, but the signal of the self in time.

Alpha Regulation and the Central Role of BA 19

Among the most studied rhythms in electroencephalography (EEG), the alpha band (8–13 Hz) has consistently emerged as a key indicator of cognitive idling, attention, and internally directed states (Barry et al., 2007; Klimesch, 1999). However, newer models suggest that alpha power, and especially its modulation, is far more than a passive index. Alpha rhythm serves as an active gatekeeper of information flow, particularly in posterior midline regions where the precuneus, posterior cingulate, and adjacent visual-parietal cortices coordinate internal simulation, self-referential thought, and attentional switching (Buckner et al., 2008; Cavanna & Trimble, 2006) as well as its interactions and involvement with the default network of the brain.

Within this network, Brodmann area 19 (BA 19), located in the medial occipital cortex, serves as a relay between visual-spatial processing and self-representational systems, especially under conditions requiring inhibitory control or internal reflection (Gusnard & Raichle, 2001). Prior work by Cannon (2009), Cannon et al. (2012, 2014, 2025), and Baldwin et al. (2011) demonstrated that this region shows significant modulation during LORETA neurofeedback (LNFB) aimed at enhancing self-regulation. Furthermore, alpha activity in BA 19 is functionally tied to posterior cingulate cortex (PCC) dynamics and medial prefrontal engagement, forming a posterior-frontal loop that we argue is essential for adaptive regulation and may be deficient in SUD populations.

Although traditionally mapped as part of the medial occipital lobe and associated with visual-spatial processing, the precuneus, especially its ventral and posterior segments, is now understood to be a key integrative hub in the DMN and a primary contributor to episodic memory, self-referential processing, and contextual awareness (Cavanna & Trimble, 2006; Leech & Sharp, 2014). Its anatomical and functional position allows it to relay and integrate sensory, cognitive, and affective information from both posterior and frontal structures. The precuneus maintains strong reciprocal connections with the PCC, which monitors self-related stimuli; the medial prefrontal cortex (mPFC), which is closely involved with value attribution, mentalizing, and emotional decision-making; the hippocampus, which supports episodic encoding; and lateral temporal and parietal regions involved in perceptual integration and social narrative continuity.

This connectivity supports what might be described as the episodic context of self, a scene-setting function that locates the self in time, space, and social position, even in the absence of external tasks. Disruptions in this region have been observed in conditions involving depersonalization, trauma, psychosis, and SUD, often presenting with unstable self-awareness, memory and identity fragmentation, or emotional disconnection (Brewer et al., 2013; Cannon et al., 2004; Northoff et al., 2006). In the context of SUD, these are not peripheral symptoms; they are core deficits. Individuals frequently experience an unstable, impoverished and fragmented self-concept, difficulty linking emotional events to behavior, and diminished access to autobiographical continuity. The precuneus may serve as a critical neural substrate for restoring a stabilized and embodied sense of self, particularly when targeted by interventions that operate within its native rhythmic domain.

Within this framework, targeting alpha modulation in the left precuneus via neurofeedback is not merely an intervention on the visual cortex, it is an intentional engagement of the brain's energetic signature of the self. This region supports contextual integration, autobiographical memory, and the temporal scaffolding of awareness. Rhythmic entrainment here may allow for reorganization of attentional control and internal coherence, offering a rare opportunity to modify the physiological substrates of self-regulation at their core. The rationale for selecting the precuneus as a neurofeedback target in previous studies with SUD subjects was twofold: first, its extensive involvement across psychiatric disorders and self-referential disturbances; and second, a more fundamental hypothesis that the DMN anchors the experience of "self." As this network rose to scientific prominence in the late 2000s, investigations of SUD in the present author's laboratory returned to a simple question: What is more default than the self? If the self holds no regulatory or reward value, then no external reinforcement will suffice. While intuitive rather than theoretical, this premise became the catalyst for a decade of work. Importantly, this line of reasoning may hold relevance for individuals with early adversity or PDE, where disruptions to the formation of self-regulatory and default network architecture have been documented well into adolescence and early adulthood (Kelley et al., 2019; Koponen et al., 2020).

In the current dataset, described below, the BA 19/precuneus pathway within the DMN was trained directly using LNFB, targeting a three-voxel cluster centered at Talairach coordinates (−31, −81, 22), corresponding to the left ventral precuneus (Cannon et al., 2014). The left precuneus was selected as the primary training target based on extensive research demonstrating its role in self-referential processing, episodic and perceptual encoding of experience, and its dense connectivity with angular and Wernicke's areas within the left parietal receptive language network, as well as its broader integration within the DMN (Buckner et al., 2008; Northoff et al., 2006).

In contrast, the right precuneus has been implicated in different functional contexts, including attentional shifts and visuospatial processing. As a precaution, particularly in populations with SUD, PTSD, and related clinical issues, we targeted the left precuneus to leverage its well-characterized role in internal mentation and language-linked integration. This choice was further supported by early alpha/theta neurofeedback work by Peniston and Kulkosky (1989), who trained at electrode site O1 and observed significant changes on Minnesota Multiphasic Personality Inventory (MMPI) scales, as well as by pilot training data demonstrating consistent modulation patterns across CSD measures, Personality Assessment Inventory (PAI) scores, and other behavioral indices when the left precuneus was trained.

What Linear Models Leave Lacking, and What Machine Learning Reveals

Traditional linear regression models assume independent, additive contributions of predictors toward a singular outcome. While these methods have served psychology and neuroscience for decades, they are inherently mismatched to the brain's recursive, interacting, and nonstationary nature (Friston, 2010). In reality, frequencies do not act in isolation, nor do regions contribute independently; rather, the brain operates as a system of rhythmic interactions that reconfigure across time and state. For neurofeedback data, especially with spatially resolved CSD features, these interactions matter far more than any single coefficient.

This is where ML offers a profound shift. Rather than testing predefined hypotheses, ML allows the data itself to reveal predictive structure. Models such as Random Forests (Breiman, 2001) are especially suited to EEG-CSD data due to their ability to handle high-dimensional, collinear, and nonlinear feature spaces. In our approach, CSD values across all ROI and alpha subbands have been used as inputs to train a classifier that could distinguish pre- from posttraining patterns or predict reliable change on an individual basis.

To interpret these models, we employed Shapley Additive Explanation (SHAP) values, a modern implementation of cooperative game theory that attributes importance scores to each input feature (Lundberg & Lee, 2017). SHAP identifies not only which regions and frequencies contribute to model predictions but also the strength and direction of these contributions. This enables us to "open the black box" of ML and clarify which aspects of neurofeedback training meaningfully drive self-regulation (Cannon, 2025).

Notably, these analytic strategies build on methods the author has used long before "machine learning" became a standard framework. Early applications included differentiating networks of executive attention in the anterior cingulate gyrus and dorsolateral prefrontal cortices (Cannon, 2009); dissertation work examining EEG sources associated with self-referential processes (Cannon, 2009); analyses of ROI-level CSD and network dynamics associated with attention task performance in ADHD (Cannon et al., 2014); and investigations of white matter connectivity disruptions between the posterior cingulate and hippocampi in Alzheimer's disease using diffusion tensor imaging (DTI) to probe episodic memory impairments (Zhou et al., 2008).

At that time, advanced statistical techniques such as logistic regression, ROC analyses, and partial correlations were employed to isolate network-level relationships, but computational and visualization workflows were slow and largely manual, often requiring image construction in PowerPoint. Contemporary SHAP-based interpretability dramatically accelerates and clarifies these kinds of multivariate network insights, allowing us to model learning dynamics at scale with far greater precision. Together, SHAP and network modeling offer a generative lens: we are not confirming theories but generating new ones from real-world change data. This is what neuroscience has long lacked, not stronger *p*-values, but stronger tools for listening to the brain as it adapts and learns.

Toward a Model of Rhythmic Self-Regulation: The Cycle of Error

Alpha activity, particularly in the posterior midline, is not simply a marker of attention or "rest." It is a

rhythmic expression of the self-regulatory system in action with an energetic signature indicating where awareness is focused, how inhibition is organized, and whether internal versus external information is being prioritized (Jensen & Mazaheri, 2010). Strikingly, few models of dopaminergic function acknowledge its role in stillness or motor inhibition, despite dopamine's well-established involvement in movement regulation (Grace, 1991). The emphasis on dopamine as a reward or drive signal has overshadowed its fundamental role in modulating motor readiness, inhibition, and behavioral gating. In this light, our approach to neurofeedback is not merely about increasing alpha, but about training the brain to flexibly shift and regulate its internal dynamics across changing contexts.

Building on previous work (Cannon et al., 2012, 2014), we conceptualize this process as a recursive cycle of error: Self-regulation often fails not because of a single discrete deficit, but through a repeating loop in which perceptual, affective, and behavioral responses mutually reinforce dysregulated states. For justice-involved individuals with SUD, this cycle of error is frequently neurodevelopmental in origin, shaped by factors such as early trauma, prenatal and perinatal substance exposure, and disrupted attachment experiences (e.g., Cannon, 2025; Cavanna & Trimble, 2006; Northoff et al., 2006). Over time, these repeating patterns become physiologically embedded through chronic enactment, leading to stable but maladaptive rhythmic and network dynamics.

The alpha system, particularly BA 19 and its cortical projections within the posterior DMN, provides a biological foothold for intervention on this repetitive cycle. By modulating rhythmic activity in the left ventral precuneus, it is possible to interrupt episodic redundancy, the brain's tendency to recycle maladaptive perceptual-affective patterns, thereby enabling the development of the scaffolding and experiential encoding necessary for a stable sense of self and improved self-regulation (Buckner et al., 2008; Cannon, 2009; Cannon et al., 2025; Zhou et al., 2008).

By identifying and targeting the energetic patterns that underlie impairments or dysregulated self-regulation, we propose that neural rhythms can be reshaped toward stability. Our use of ML is central to this goal: rather than manually categorizing responders or cherry-picking outcomes, we train models to identify the structure of learning itself. SHAP values help reveal which regions participate most meaningfully. Also crucial to our work is the use of Principal Components Analysis (PCA), described below, which shows how group-level change emerges, and Reliable Change Index (RCI) which quantifies whether these shifts are clinically and statistically meaningful on the individual level (Jacobson & Truax, 1991).

Importantly, prior observations and theoretical considerations suggest that increased alpha activity is not uniformly beneficial. In some individuals, reliable alpha desynchronization has been associated with positive behavioral change, reflecting the possibility that neural downregulation and disengagement from maladaptive patterns may be a necessary prelude to stabilization. If so, ML methods may help clarify these response profiles, revealing when and for whom up- or downregulation of rhythmic activity supports adaptive self-regulation. Such flexibility challenges earlier neurofeedback models that often treated "more power is better" as an implicit assumption, rather than a tested principle.

Study Aims

In this paper, we present a dataset of 63 incarcerated individuals with SUD who completed LNFB training at the left precuneus (BA 19), alongside pre–post PAI measures and voxel-wise CSD data (Cannon et al., 2025). We use Random Forests to model self-regulation outcomes and SHAP values to interpret model dynamics. We present new network evidence of posterior-to-frontal alpha redistribution and confirm reliable changes through both RCI classification and PCA.

Our overarching aim is to demonstrate that ML-driven neurofeedback can (a) uncover meaningful regulatory subtypes, (b) detect both synchronization and desynchronization learning profiles, and (c) support a dynamic model of rhythmic self-regulation in vulnerable clinical populations. Crucially, these approaches move beyond linear pre–post comparisons and toward modeling network-level change, capturing the distributed, nonlinear, and state-dependent dynamics of brain adaptation (Sitaram et al., 2017). We argue that ML and AI are not only valuable for analyzing LORETA-based protocols but essential for advancing the entire field of neurofeedback. Surface-level protocols such as SMR or alpha-theta training have long demonstrated behavioral and clinical impact yet lack corresponding cortical models that explain how or where these changes occur (Haugg et al., 2020). While MRI and EEG studies have revealed connectivity changes following surface neurofeedback, these findings remain difficult to translate into individualized

treatment models. Yet in much contemporary brain research, even when statistically significant group effects are reported, we rarely ask a critical question: What magnitude of power or connectivity change actually constitutes a meaningful effect on system-wide or behavioral outcomes? This gap has become especially urgent in light of the broader replication crisis, which has shown that many statistically significant findings fail to replicate or translate into real-world contexts (Ioannidis, 2018; Open Science Collaboration, 2015).

Our approach, employing individualized neurofeedback training, CSD metrics, and ML, is designed to help bridge this gap, shifting emphasis from abstract statistical significance toward measurable, reproducible neural change that corresponds with behavioral outcomes.

Without robust tools to decode the functional architecture behind training, much of neurofeedback has remained protocol-driven rather than network-driven. ML and AI now offer the opportunity to reverse this, allowing us to detect, predict, and ultimately prescribe training protocols based on meaningful neurophysiological features. This study represents one step in that direction, anchoring protocol design in rhythm, region, and recovery, not just in surface targets or statistical significance.

Methods

Participants

This case grouping includes 63 individuals (19 female) with a mean age of 37.11 (*SD* = 9.69), 58 of whom were right-handed. The initial participant count was 110, with 64.5% completing the protocol and 35.5% dropping out. Only those who completed all sessions, as well as post-LNFB baseline and PAI measures, were included in the final analysis. Inclusion criteria included a history of substance-related legal offenses and willingness to participate in a 20-session neurofeedback training protocol. All participants completed pre- and posttraining psychometrics and EEG recordings from (Cannon et al., 2025).

Neurofeedback Protocol

Participants underwent 20 consecutive sessions of alpha uptraining, and their brain activity was measured via CSD extracted from LORETA source space. CSD offers an anatomically constrained estimate of energy dynamics in microamps per square centimeter (μA/cm²), allowing for precise, frequency-specific insights at both the voxel and region level (Pascual-Marqui et al., 1994, 2002). LNFB training sessions were composed of six 5-min rounds and were conducted five times per week for 20 consecutive weekdays. For each session ~3-min presession eyes-opened baselines were collected. Each session required ~50 min to complete. In the preliminary session, the participants were instructed to control tongue and eye movements, blinks, and muscle activity in forehead, neck, and jaws. This enabled the subjects to minimize the production of extracranial artifacts, in electromyography (EMG), electro-oculogram (EOG), etc., during the sessions. During the preliminary session shaping was induced to set thresholds such that each participant could meet the reward criteria of 20 points per minute at a minimum (e.g., generate the desired response at a minimal rate), and participants were informed of the inhibitory and reward aspects of the training. Standardized thresholds listed below were then set and maintained for each participant (Cannon, 2014; Cannon et al., 2014, Cannon et al., 2025). Participants were able to choose from a selection of 25 games for the sessions. The participants were provided visual and auditory feedback, and points were achieved when they were able to simultaneously increase alpha CSD (8–13 Hz) at the, left precuneus while minimizing EMG (35–55 Hz) and EOG (1–3 Hz) in linear combinations of channels: EMG: T3, T4, T5, T6, O1, and O2; EOG: FP1, FP2, F3, F4, F7, and F8. These criteria had to be maintained for .75 s to achieve 1 point. The auditory stimuli provided feedback with a pleasant tone when the criteria were met. Similarly, the visual stimuli were activated when the criteria were met (e.g., a car or a spaceship driving faster and straighter). Alternatively, slower speed of the car, driving in the wrong lane, or the spaceship flying slowly and crookedly were seen when the criteria were not met (Deymed Diagnostics). The score for meeting the criteria was also seen by the participants in a small window of the game screen. Additionally, the visual stimuli contained a signal for rewards and inhibits relative to a threshold level, and a bar graph illustrating reward, EOG and EMG. After completing at least 10 sessions without missing any sessions without a valid excuse (illness, court, etc.), inmates were permitted to use DVD movies for the A/V feedback mechanism. The DVD covaries with the inhibit and reward features by the sound diminishing or the screen being blurred or noise added when the criteria are not met.

EEG Recording and CSD Extraction

EEG was recorded using a 21-channel gel-based cap (10–20 system) with a sampling rate of 256 Hz. Channels included Fpz, Fp1/2, F3/4, C3/4, P3/4, O1/2, and midline sites (Fz, Cz, Pz). Reference was

set to linked ears, and impedance was maintained below 15 kΩ.

In contrast with studies utilizing traditional neurofeedback, the whole-head EEG data with 19 electrodes were continuously stored during the sessions. In addition, the participants in this study were encouraged to keep a written journal of sleep patterns, mood, overall cognitive and attention processes, and to note specifically any odd occurrences. EEG data for all participants were analyzed at premeasures and across each session with NeuroGuide (Applied Neuroscience, Tampa, FL) and contrasted to normative samples in the lifespan database to examine power metrics and connectivity across sessions during training However, for pre- and postcontrasts NeuroGuide was employed for the automatic artifact identification procedures that were utilized for gross artifact contamination, then EEG data were converted to Lexicor format and edited with EureKa!3 software by NovaTech EEG (Mesa, AZ). All EEG data were processed with particular attention given to the frontal and temporal leads. All episodic blinks, eye movements, teeth clenching, jaw tension, body movements, and possible electrocardiogram (EKG) were removed from the EEG stream by visual inspection. For all included sessions, power spectra were computed using fast Fourier transform (FFT) over 75% overlapping 4-s epochs, and log-transformed spectral densities were obtained prior to modeling. The 10 ROI were selected based on prior findings (Cannon, 2009; Cannon et al., 2012) and potential hubs of the self-regulation network. A full list of coordinates and anatomical labels is presented in Table 1. These cross-spectral matrices constitute the input for LORETA estimation in the frequency domain. CSD was then computed using standardized LORETA (Pascual-Marqui, 2002; Pascual-Marqui et al., 1994) at each of 10 predefined cortical ROI. Spectral CSD estimates were averaged within six frequency bands: delta (1–4 Hz), theta (4–8 Hz), alpha1 (8–10 Hz), alpha2 (10–13 Hz), beta1 (13–21 Hz), and beta2 (21–40 Hz). ROI-level averages were used as input features for ML and statistical analysis.

Psychological Assessment

The PAI (Morey, 1991) was administered pre- and posttraining. The PAI is an objective inventory of adult personality characteristics that assesses psychopathological syndromes and provides information relevant for clinical diagnosis, treatment planning, and screening for psychopathology. This assessment contains 344 items that constitute 22 nonoverlapping scales covering the constructs most relevant to a broad-based assessment of mental disorders: four validity scales, 11 clinical scales, five treatment scales, and two interpersonal scales. To facilitate interpretation and to cover the full range of complex clinical constructs, 10 scales contain conceptually derived subscales. The scales (with subscales in parentheses) listed in the table are somatic (conversion, somatization, health concerns); anxiety (cognitive, affective, physiological); anxiety related disorders (obsessive-compulsive, phobias, traumatic stress); depression (cognitive, affective, physiological); mania (activity level, grandiosity, irritability); paranoia (resentment, hypervigilance, persecution); schizophrenia (psychotic experiences, social detachment, thought disorder); borderline features (affective instability, identity problems, negative relations, self-harm); antisocial features (antisocial behaviors, egocentricity,

Table 1

Regions of Interest for Analytics and Machine Learning Procedures

x	*y*	*z*	Region	Label	BA	#
5	0	35	Limbic Lobe	Cingulate Gyrus	BA 24	ROI 9
15	−85	0	Occipital Lobe	Lingual Gyrus	BA 17	ROI 8
40	−5	10	Sub-lobar	Insula	BA 13	ROI 7
25	55	5	Frontal Lobe	Superior Frontal Gyrus	BA 10	ROI 6
−10	−50	30	Parietal Lobe	Precuneus	BA 31	ROI 5
−15	−60	5	Limbic Lobe	Posterior Cingulate	BA 30	ROI 4
−5	0	35	Limbic Lobe	Cingulate Gyrus	BA 24	ROI 3
−15	−85	0	Occipital Lobe	Lingual Gyrus	BA 17	ROI 2
−30	30	35	Frontal Lobe	Middle Frontal Gyrus	BA 9	ROI 1
−25	−75	10	Occipital Lobe	Cuneus	BA 30	ROI 0

Note. In the SHAP images and tables ROI 0 = ROI 1 and ROI 9 = ROI 10.

stimulus-seeking); aggression (aggressive attitude, verbal aggression, physical aggression). Delta scores (post–pre) were computed for all clinical subscales, entered into ML models, and used to interpret state change.

RCI Derivation and Application

To determine whether observed changes in neurophysiological signals following LNFB training represented meaningful effects beyond measurement error, we applied the RCI framework (Jacobson & Truax, 1991). The RCI is a well-established method for distinguishing true change from statistical noise. However, due to the absence of normative CSD baselines in substance-using populations and across specific Brodmann area–defined ROI, standard reliability-adjusted formulas could not be universally applied.

Log-transformed CSD values were used in all RCI computations to normalize amplitude distributions and reduce outlier distortion. Empirical mean and *SD* were calculated per ROI using the pre- and posttraining eyes-opened baseline data for all completers. While normative test–retest databases for CSD remain limited in SUD populations, our choice of internal standardization mirrors recent RCI applications in small-sample biobehavioral research.

Instead, the RCI was derived using empirical means and standard deviations from our study sample, following a simplified but validated approach:

$$RCI = \frac{X_{post} - X_{pre}}{SD_{pre}}$$

Where:

- X_{pre} = log-transformed CSD value at baseline
- X_{post} = log-transformed CSD value posttraining
- SD_{pre} = standard deviation of pretraining values across participants for that ROI

This method is supported by prior research demonstrating high test–retest reliability of log-transformed CSD values. Specifically, Cannon et al. (2012) reported reliability coefficients exceeding .90 for current density at both the precuneus and anterior cingulate cortex over a 30-day interval, confirming the temporal stability of these signals in nonclinical populations. These findings support the use of within-sample variance estimates when external normative data are unavailable.

We adopted a bidirectional threshold of |RCI| > 1.96 |RCI| denoting change at or beyond the 95% confidence interval. This threshold was used to classify participants as “increase responders,” “decrease responders,” or “nonresponders” at each ROI, capturing both synchronization and desynchronization effects across training.

This empirical RCI framework may also offer a generalizable approach for evaluating signal-level change in other neurophysiological or biochemical measures where normative or test–retest data are sparse. By grounding change metrics in sample-derived variance, researchers can apply this method across small-sample or early-phase interventions, including EEG, fMRI, heart rate variability, or inflammatory markers—domains where pre–post comparison is often the most feasible index of treatment response. As such, the present model contributes to a broader push for rigorous, individualized metrics of change in applied neuroscience and biobehavioral research.

Machine Learning Workflow

A Random Forest classifier (Breiman, 2001) was trained to predict reliable alpha change using input features derived from pre- and posttraining CSD values and PAI deltas. Data were preprocessed using Python 3.11 and Scikit-learn v1.4.1. Log-transformed CSD values were computed for 10 ROI at alpha and theta frequencies. Delta PAI scores (post–pre) were included as behavioral features, and RCI group labels were used as binary or multiclass outcomes depending on the model. Model training was conducted in Python using Scikit-learn with default hyperparameters (n_estimators = 100, max_depth = auto). Accuracy and feature importance were evaluated using cross-validation.

SHAP values (Lundberg & Lee, 2017) were used to interpret model output and estimate the relative contribution of each ROI and frequency band. SHAP values were averaged across trees to produce global feature importance scores and visualized via summary plots.

To mitigate overfitting and ensure generalizability, we implemented several key safeguards throughout our ML workflow. First, ROI-level CSD data were log-transformed prior to model input to reduce skew and minimize the influence of outliers or inflated amplitude values. Second, feature dimensionality

was constrained by using region-averaged CSD within specific frequency bands rather than voxel-wise inputs, reducing noise and multicollinearity. Third, we employed a Random Forest classifier, chosen for its resilience to collinearity and capacity for internal feature selection (Breiman, 2001). Fourth, cross-validation was applied across training folds to prevent overfitting and evaluate model stability. Finally, SHAP values were used to interpret feature importance and verify that biologically plausible effects—not artifacts—were driving model predictions. These combined steps provide strong assurance that our findings reflect robust, generalizable signal rather than overfit noise or conflated variance.

Principal Component Analysis (PCA)

To examine clustering and dimensional compression, PCA was applied to the full matrix of alpha band CSD values (pre- and posttraining) across all subjects. The first two principal components (PC1 and PC2) were retained for visualization. Subjects were color-coded based on RCI classification and plotted to examine response-based grouping.

All preprocessing, classification, and visualization code was developed in Python 3.11.8 using open-source packages. Analytic notebooks and deidentified data matrices are available upon request for academic replication. A reproducible pipeline for CSD transformation, RCI classification, and Random Forest modeling is currently being prepared for public release.

Results

CSD Network Patterns and Posterior–Frontal Shift

Posttraining CSD values revealed consistent energy redistribution across posterior and frontal ROI. Figures 2 and 3 show the results for paired contrasts with significant alpha1 and alpha2 increases at the target ROI ($p < .05$), with secondary modulation observed in left anterior cingulate (ROI 3) and midline posterior cingulate (ROI 4) regions. A regression-weighted network diagram (Figure 4) illustrates a posterior to frontal shift in spectral alpha activity, interpreted as enhanced engagement of top-down regulatory networks.

Figure 2. *Deltas for CSD Levels in Posterior/Frontal Regions Linked to Precuneus Training Region.*

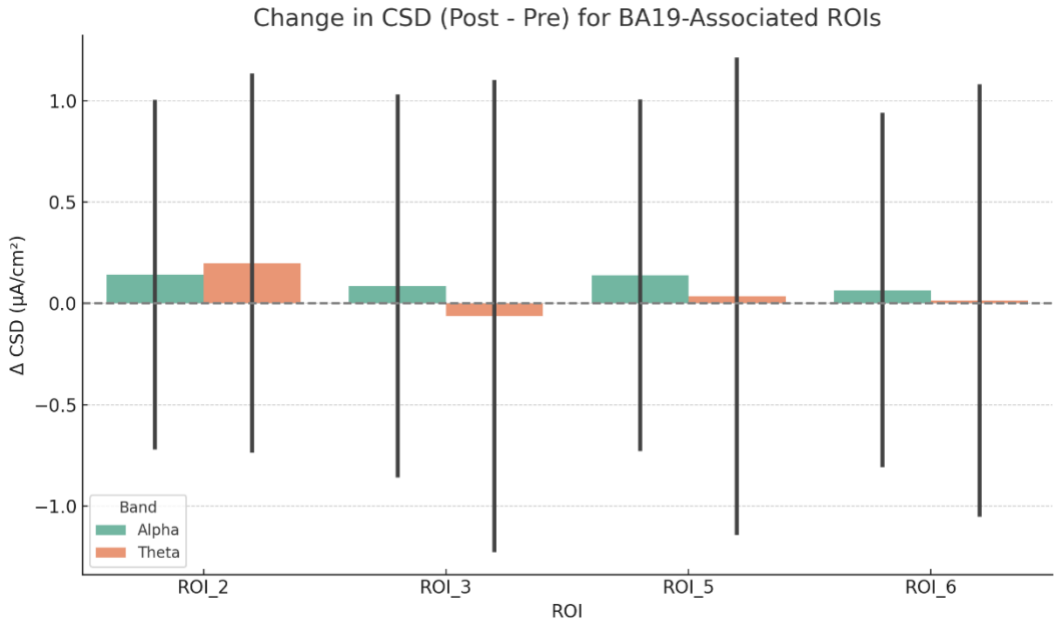

Figure 3. *Deltas for CSD in Frontal Regions Tied to SR and Posterior Regions.*

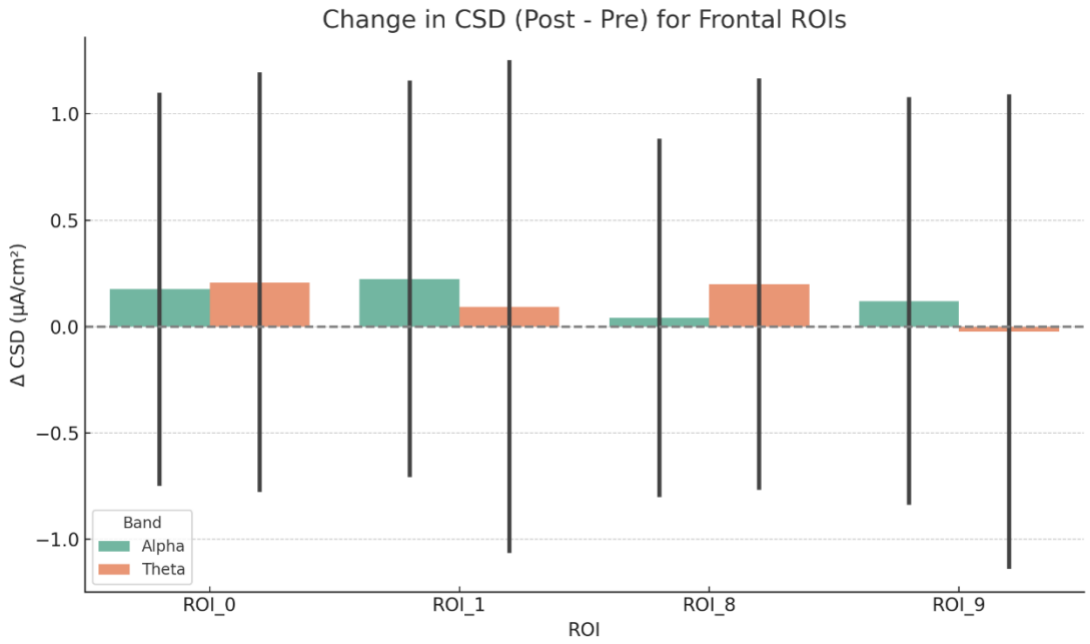

Figure 4. *Directed Posterior → Frontal Network Based on ΔAlpha CSD Regression Paths (N = 63).*

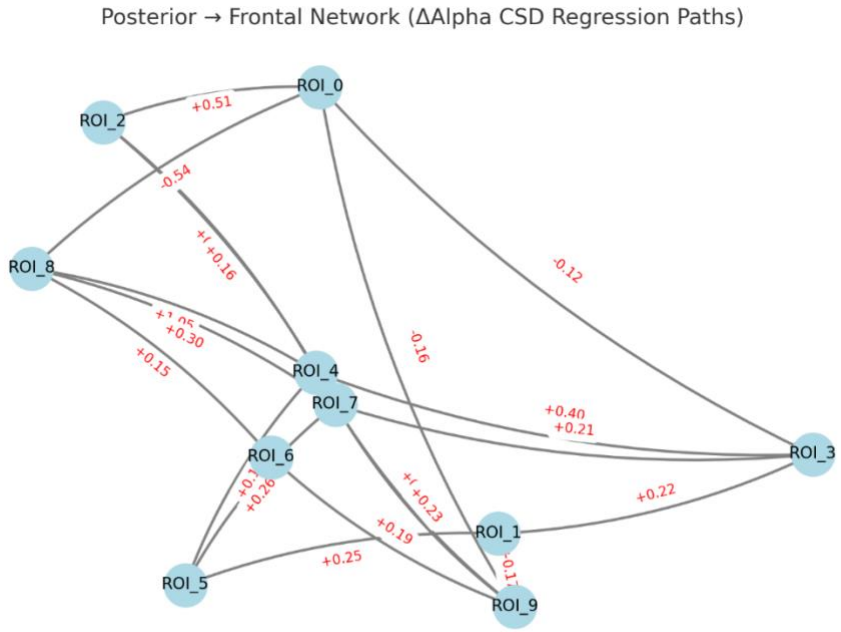

Note. Line sizes indicate significant directional relationships (|β| > 0.10) from posterior to frontal ROI. Node labels represent ROI indices. Edge labels within the figure reflect standardized beta coefficients (Table 2) derived from multiple linear regressions using posterior ROI predictors.

Network-level correlation analysis revealed a structured set of associations between alpha-band CSD shifts and changes in PAI symptom domains (Figure 5). Notably, ROI_4 (Posterior Cingulate) and ROI_2 (Lingual Gyrus) emerged as central hubs, showing multiple strong positive correlations (red) with clinical deltas—especially for somatic complaints, paranoia, and antisocial traits. Negative associations (blue) were more prevalent, consistent with symptom reduction accompanying increased alpha power in key posterior ROI. This pattern further supports the model that alpha synchronization within posterior visual-parietal areas contributes to broad symptom stabilization, particularly within self-perceptual and threat-related domains.

Compared to the alpha-based network, the theta-band model (Figure 6) exhibited a broader and denser matrix of negative associations between neural and clinical change. Posterior cingulate/precuneus (ROI_5) and lingual gyrus (ROI_4) remained active hubs, while ROI_2, a ventral occipital/BA19 contributor, also emerged as highly connected. The majority of associations were negatively signed, suggesting that increased theta synchronization was linked with symptom reductions —especially in scales indexing somatic, depressive, and paranoid ideation. These results imply that theta dynamics may reflect a regulatory substrate, enabling attenuation of maladaptive internal states and ruminative traits.

The composite network (Figure 7) illustrates a convergent and distributed structure linking CSD changes at posterior ROI with improvements across diverse symptom domains. Notably, purple edges (shared alpha and theta) clustered around aggression (agga_d), somatic complaints (somc_d), and perceptual disturbance (sczt_d), confirming that both frequency bands engage shared regulatory circuits. Theta-specific (orange) associations dominated paranoia, mania, and anxiety subscales, while alpha-specific (green) links concentrated around cognitive and interpersonal traits. These patterns support a dual-frequency model of neuroplastic change, with alpha coordinating internal sensory regulation and theta modulating affective-cognitive integration.

Figure 5. *Alpha-Band ROI-to-PAI Delta Network Showing Significant Correlations Between Alpha-Band CSD Changes at Selected ROI and Changes in PAI Symptom Scores (|r| ≥ 0.20).*

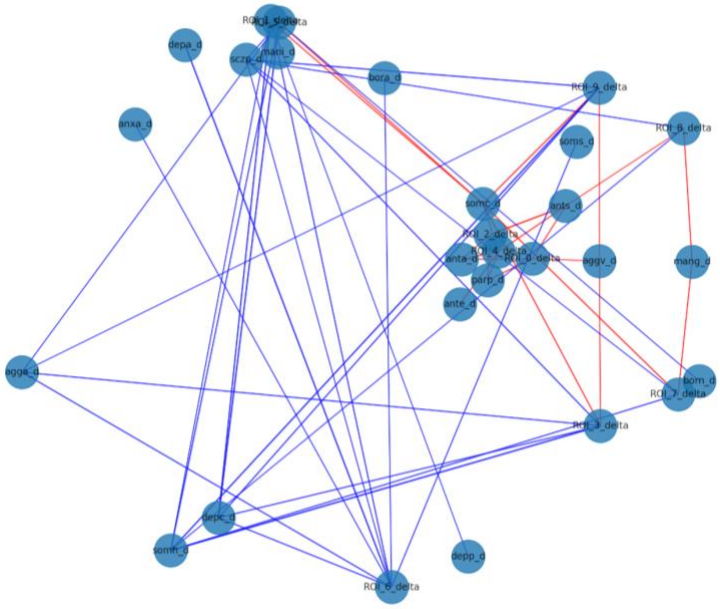

Note. Nodes represent either a PAI subscale delta (e.g., somc_d) or an ROI delta (e.g., ROI_4_delta). Blue edges indicate negative correlations; red edges indicate positive correlations. Edge thickness reflects the strength of association. Central nodes include ROI_2, ROI_4, and somc_d, highlighting convergence between posterior alpha modulation and somatic/cognitive symptom resolution.

Figure 6. *Theta-Band ROI-to-PAI Delta Network Showing Significant Correlations (|r| ≥ 0.20) Between Theta CSD Changes Across ROI and PAI Symptom Change Scores.*

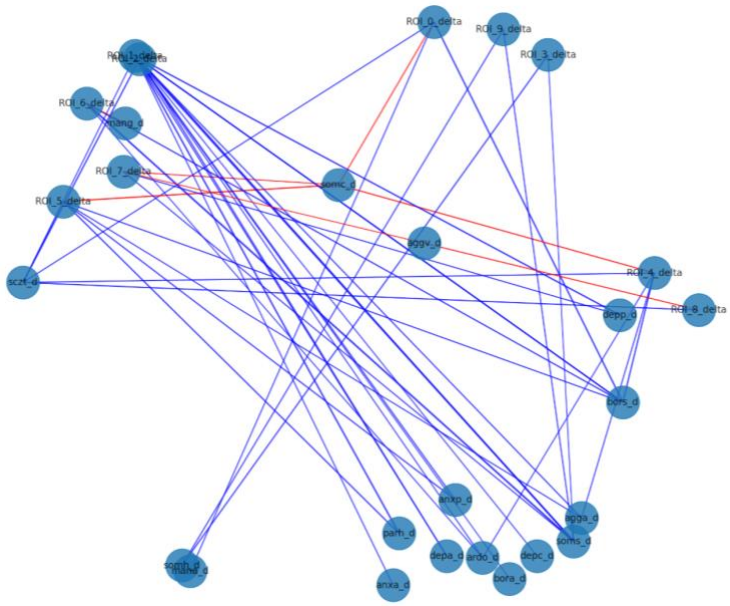

Note. Blue edges represent negative correlations (improvement associated with increased theta CSD); red edges indicate positive correlations. Several posterior ROI (e.g., ROI_4, ROI_5, ROI_0) demonstrate high degree centrality, linking with changes in diverse PAI subscales including aggression, somatic complaints, and depression.

SHAP Interpretation of Predictive Features

SHAP summary values in Figure 4 revealed that posterior (ROI 2, ROI 5) and left frontal (ROI 3) alpha bands contributed most to the model's predictions. Alpha2 (10–13 Hz) in ROI 2 and alpha1 (8–10 Hz) in ROI 3 had the highest positive impact on model output, aligning with the observed functional connectivity pathway. Notably, desynchronization responders showed SHAP profiles with inverse contributions in ROI 4, suggesting differential strategies in regulation. SHAP summary plots were generated using the TreeExplainer module from the SHAP package (v0.41.0), with line size by frequency and ROI for interpretability. Table 2 shows the region, target ROI and beta coefficients for the model. Dependence plots were also used to probe nonlinear effects and ROI–frequency interactions.

Alpha CSD Change and RCI Classification

Because ROI 5 (left ventral precuneus, BA 19) and frontal midline regions, primarily anterior cingulate cortex (ACC; BA 24/32) and mPFC (BA 10/11), are key nodes within the self-regulation network, we classified participants based on reliable alpha modulation (|RCI| > 1.96) observed at these posterior and frontal sites. Participants were categorized as dual responders when reliable modulation occurred at both ROI 5 and the frontal ROI, frontal-only or precuneus-only responders when change was isolated to one region, and nonresponders when neither site met the threshold.

Out of the 63 participants, 21 individuals (33.3%) demonstrated reliable alpha modulation at both the precuneus and frontal ROI, qualifying them as dual responders. Another 10 participants (15.9%) exhibited reliable change only at the frontal ROI, while 8 participants (12.7%) showed reliable modulation exclusively at the trained precuneus site. The remaining 24 participants (38.1%) did not meet the threshold for reliable change at either site and were classified as nonresponders.

Figure 7. *Combined Alpha and Theta Band ROI-to-PAI Delta Network Showing All Correlations ≥ 0.20.*

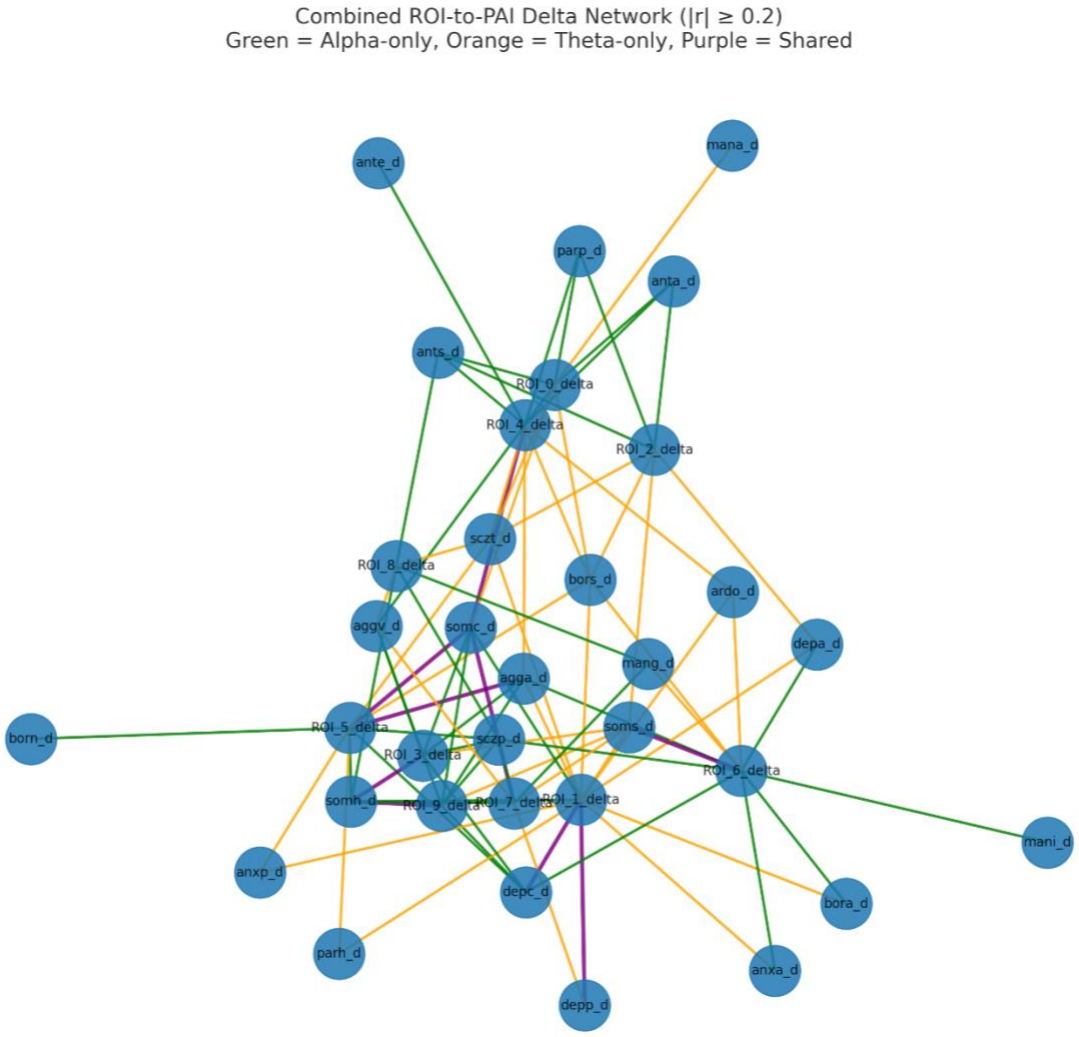

Note. Green edges represent alpha-only associations; orange edges indicate theta-only associations; and purple edges indicate correlations observed in both bands. Nodes represent ROI or PAI symptom delta variables. Shared associations (purple) highlight cross-frequency contributions to key symptom changes, particularly somatic complaints, aggression, and thought disorders.

Table 2

Regression Path Coefficients for Directed Posterior → Frontal ROI Network (ΔAlpha CSD)

Source Region (ROI)	Target Region (ROI)	Standardized Beta
Cuneus (ROI_0)	Cingulate Gyrus BA24 (ROI_3)	−0.12
Lingual Gyrus (ROI_1)	Cingulate Gyrus BA24 (ROI_3)	+0.22
Lingual Gyrus (ROI_4)	Cingulate Gyrus BA24 (ROI_3)	+0.21
Posterior Cingulate (ROI_6)	Cingulate Gyrus BA24 (ROI_5)	+0.19
Precuneus (ROI_7)	Cingulate Gyrus BA24 (ROI_5)	+0.26
Lingual Gyrus (ROI_1)	Insula (ROI_9)	−0.17
Precuneus (ROI_7)	Insula (ROI_9)	+0.25
Cuneus (ROI_0)	Middle Frontal Gyrus (ROI_2)	+0.51
Lingual Gyrus (ROI_4)	Middle Frontal Gyrus (ROI_2)	+0.16
Cuneus (ROI_0)	Superior Frontal Gyrus (ROI_8)	+0.54
Lingual Gyrus (ROI_4)	Superior Frontal Gyrus (ROI_8)	+0.30
Posterior Cingulate (ROI_6)	Superior Frontal Gyrus (ROI_8)	+0.15
Precuneus (ROI_7)	Superior Frontal Gyrus (ROI_8)	+1.05

Note. Standardized beta coefficients for each significant regression path (|β| > 0.10) from posterior to frontal regions of interest (ROI) based on change in alpha band current source density (ΔCSD). ROI codes correspond to the functional-anatomical areas introduced in Table 1.

This distribution reveals that more than 60% of participants demonstrated physiologically meaningful change across one or both targeted regions, with a substantial portion engaging both posterior and frontal self-regulatory structures. These outcomes further support the idea that neurofeedback training at the precuneus initiates broader network-level reorganization. The distribution of response types is presented in Figure 8.

Analysis of PAI delta scores revealed clear and distinct patterns of change across Alpha RCI-defined responder types. Figure 9 illustrates the 15 PAI subscales with the greatest between-group variation. Individuals classified as precuneus-only responders demonstrated the most robust and consistent positive changes across several clinically meaningful subscales, including features related to paranoia (parp_d; paranoia), borderline (bori_d; identity), aggression (aggp_d; physical aggression), and anxiety (anxa_d; affective).

Dual responders showed moderate improvements across many domains, including (anxc_d; cognitive), schizophrenia (sczp_d; psychotic), and somatic complaints (somc_d; conversion). In contrast, Frontal-only responders displayed more selective change, particularly in cognitive-related domains such as schizophrenia-thought disorder (sczt_d; thought disorder) and antisocial traits (anta_d; antisocial behaviors), while nonresponders consistently exhibited the least overall delta and narrower variability across all subscales.

Frontal-only responders demonstrated a marked and unexpected increase on the Mania grandiosity subscale (mang_d; grandiosity), with an average delta of nearly +15 points, which is substantially higher than any other group. This isolated elevation may reflect superficial cognitive compensation or defensive restructuring, potentially triggered by early-stage frontal activation in the absence of deeper self-referential integration. Without concurrent modulation of posterior regions such as the precuneus, these frontal changes may lack grounding in experiential processing or introspective awareness. This finding underscores the importance of whole-network training approaches for producing balanced and enduring psychological change.

Figure 8. *Classification of RCI Response Types in the SUD Participant Group (N = 63), Using Absolute RCI Threshold of |1.96|.*

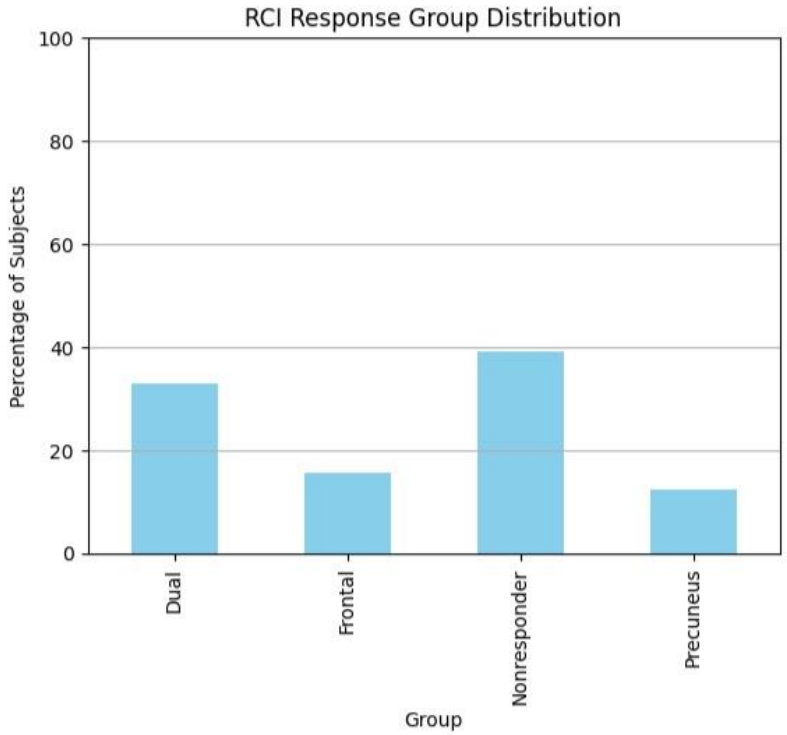

Note. Subjects were grouped into four categories: Dual Responder (alpha change at both frontal and precuneus ROI), Precuneus Only, Frontal Only, and Nonresponder. This classification reflects clinically meaningful alpha modulation regardless of direction, supporting functional interpretation of both increase and desynchronization responses.

Figure 9. *Mean PAI Delta Scores Showing the Greatest Between-Group Differences Across Alpha RCI-Defined Response Types (SUD Group, N = 63).*

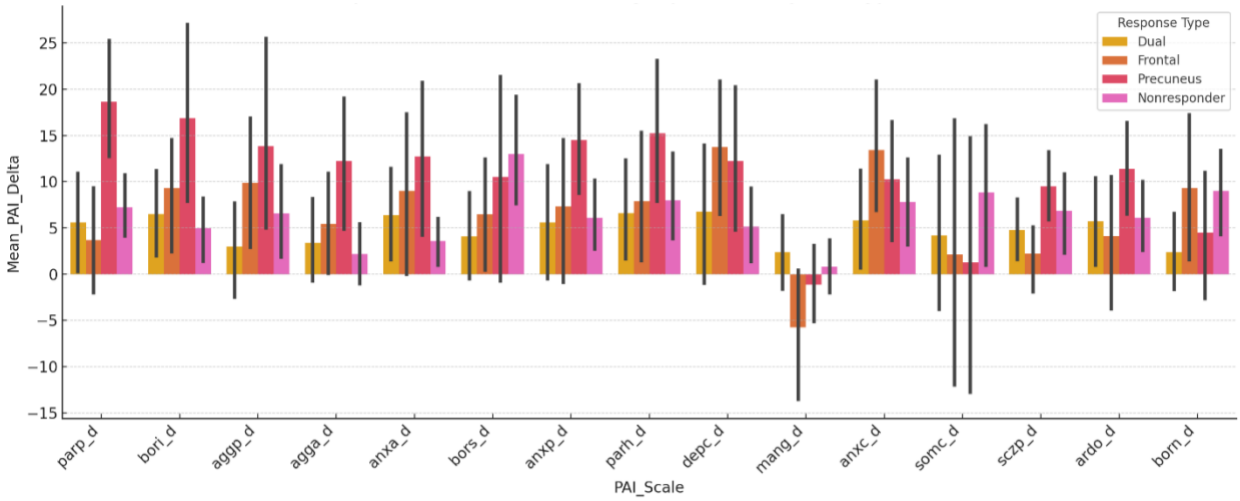

Note. Groups include dual responders (change at both frontal and posterior alpha ROI), frontal-only responders, precuneus-only responders, and nonresponders. Bars represent mean change scores from pre- to posttraining, with error bars denoting standard error of the mean. The subscales reflect clinical domains such as paranoia persecution, aggression physical, anxiety affective, and schizophrenia thought disorder. Precuneus responders exhibited the strongest improvements across multiple domains.

PAI Delta Scores and Behavioral Change

Group-level PAI deltas indicated consistent reductions in subscales of aggression (AGG) related to somatic issues, cognitive and affective components, and to the affective instability subscale of the borderline scale (BOR) across all RCI groups. Both increase and desynchronization responders showed greater magnitude of change compared to nonresponders. Exploratory analysis showed that desynchronization responders exhibited larger reductions in somatic and aggressiveness subscales, even during incarceration, potentially reflecting a deactivation of maladaptive frontal overdrive.

SHAP analysis was performed to identify which brain regions and frequency bands most strongly predicted changes in personality symptomatology (PAI delta scores) following LNFB. Figure 10 illustrates the most significant ROI for both alpha and theta frequency bands, based on mean SHAP values from the trained Random Forest model.

The most significant alpha predictor was ROI 8 (left occipital/lingual gyrus), which yielded a mean SHAP value approaching 4.0, indicating a substantial role in forecasting PAI score improvement. This was followed by ROI 6 (superior frontal) and ROI 1 (middle frontal), both of which contributed meaningfully to model predictions. Theta-band predictors were led by ROI 5 (posterior cingulate/precuneus), which showed the highest SHAP value across all theta features, followed by ROI 6 and ROI 9 (right ACC).

The distinct frequency-specific ranking underscores the complementary roles of alpha and theta rhythms in shaping individual psychological trajectories. Alpha dynamics were particularly influential in frontal and parietal regions associated with regulation, attention, and cognitive control. Theta contributions were more prominent in limbic and midline structures, suggesting involvement in emotional reactivity and internal narrative modulation.

Together, these findings support the idea that the integration of both alpha and theta rhythms is important in modeling personality change, reinforcing the view that multiple frequency-specific mechanisms underpin neurofeedback-related improvement in complex clinical populations.

PCA Visualization of Learning Clusters

PCA was conducted on the full matrix of alpha and theta CSD change scores across all ROI to examine the dimensional structure of training-related brain dynamics. The first two principal components (PC1 and PC2) captured the majority of shared variance across subjects and frequency bands, providing a compressed representation of network-level change. The alpha/theta PCA model achieved an R^2 of approximately 0.72 with a correspondingly low RMSE (~0.0019), indicating strong model fit without evidence of overfitting. Given that this represents an initial stage of ML/AI implementation on a novel dataset and analytic pipeline, these values are expected to improve with larger samples and more sophisticated model tuning, thereby enhancing the predictive power of the framework. As shown in Figure 11, PCA revealed partially overlapping but distinct distributions of alpha and theta responses. While both frequency bands occupied a shared low-dimensional space, their relative spread suggests differential encoding of treatment effects. Theta-band CSD changes were more laterally distributed along PC1, whereas alpha responses tended to separate vertically along PC2. This divergence implies that the two bands contribute complementary information: theta may reflect broader network synchrony or state-related variability, while alpha appears more associated with targeted regulation and intra-individual modulation.

To examine the spectral and spatial precision of neurofeedback effects, Cohen's d was computed for post–pre differences in CSD amplitude across 20 frequency bins for four BA 19-associated ROI including frontal ROI (ROI 2, ROI 3, ROI 5, ROI 6).

As shown in Figure 12, the largest effect sizes clustered in the alpha band (8–13 Hz) and its neighboring bins, confirming the specificity of modulation to the trained frequency range. These effects were most prominent in ROI 3 and ROI 5, supporting both the SHAP-derived frontal importance and the posterior–frontal redistribution observed in network-level modeling.

Frequency-resolved effect size mapping revealed ROI- and bin-specific patterns of CSD modulation. ROI6 (Superior frontal gyrus) exhibited a peak positive effect in the highest frequency bin (Bin_20), reflecting increased gamma-range CSD, while also showing consistent modulation across alpha and beta ranges. Conversely, ROI3 (anterior cingulate) demonstrated notable suppression in low-frequency bins (Bins 3–5), consistent with desynchronization in theta during neurofeedback.

Figure 10. *ROI of Greatest Significance for Predicting PAI Delta Scores, Derived From SHAP Values in Random Forest Models Using Alpha and Theta Band CSD as Input Features.*

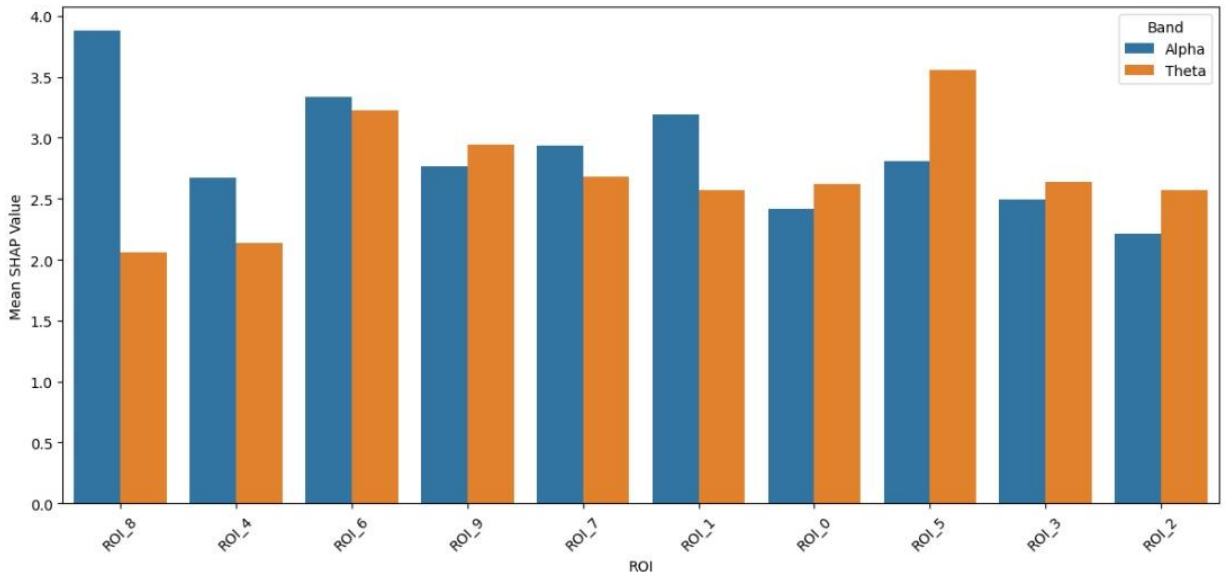

Note. ROI are sorted by overall contribution, with separate bars for alpha (blue) and theta (orange). ROI 8 (left frontal cortex) showed the highest SHAP value for alpha, while ROI 5 (posterior cingulate) was the most predictive in the theta band. This suggests frequency- and region-specific contributions to personality change following neurofeedback.

Figure 11. *PCA of Total CSD Change Across All ROI, Separated by Frequency Band.*

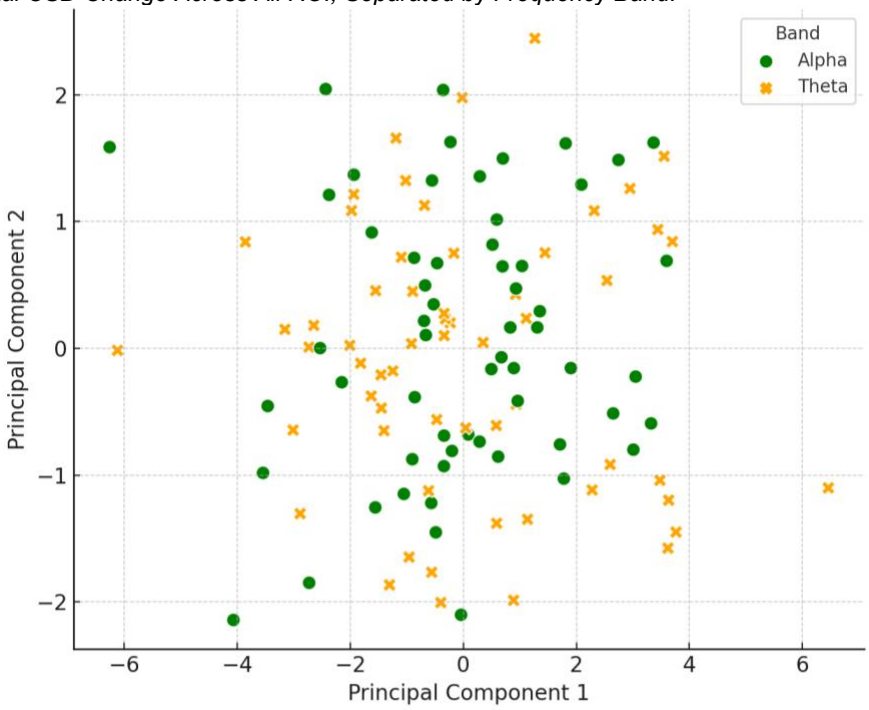

Note. Each point represents a subject's CSD change profile projected into 2D PCA space for the alpha (green) or theta (orange) band. Principal components reflect major axes of variance in neurophysiological change patterns. Overlap in distributions suggests shared underlying structure, while band-specific dispersion may indicate distinct frequency-resolved response characteristics.

Figure 12. *Effect Sizes (Cohen's d) for CSD Change From Pre- to Posttraining Across Four BA 19-Related ROI and 20 Frequency Bins (Each Spanning 2 Hz From 1–40 Hz).*

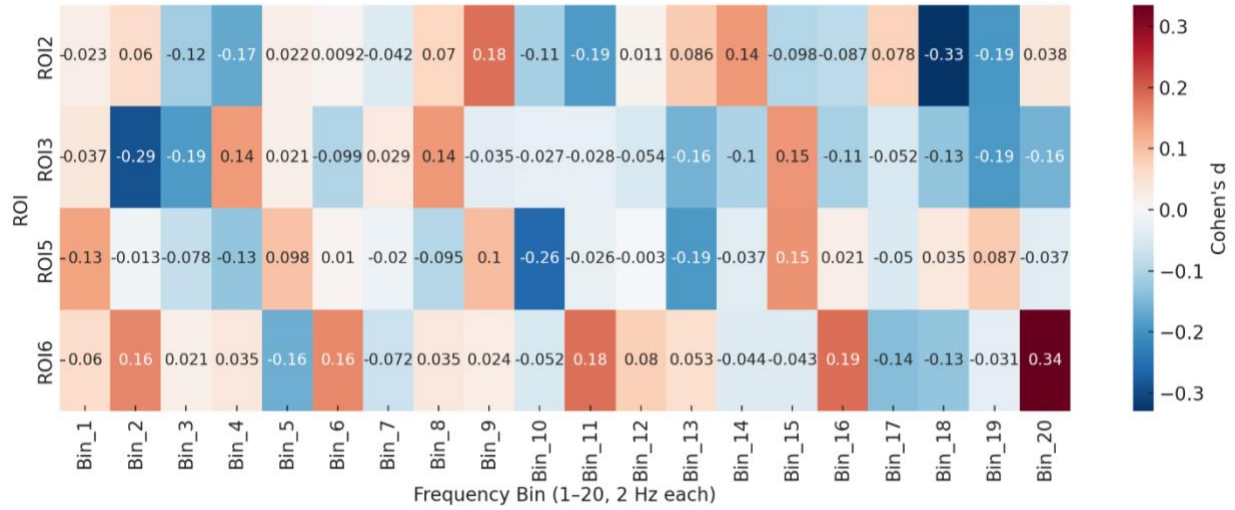

Note. Positive values (red) indicate increased posttraining CSD; negative values (blue) indicate reduced CSD. ROI labels reflect Brodmann area 19 subregions (e.g., ROI2: Cuneus; ROI3: Lingual Gyrus; ROI5: Posterior Cingulate; ROI6: Precuneus). ROI6 (Precuneus) showed the strongest increase in the 39–40 Hz bin, while ROI3 exhibited consistent suppression across low-mid frequencies.

Discussion

This study was not designed to validate or disprove theoretical models, nor to retest hypotheses already well-established in linear EEG or clinical outcome literature. Those studies have been done and often leave more questions than answers when applied to real-world, high-risk populations. Instead, we approached this analysis with a simple but essential question: What, if anything, is changing in the brain of someone with a SUD when they undergo targeted LNFB at the precuneus? And to inform regarding the questioning of neurofeedback training in general—what specific effects are shown from neurofeedback training?

Rather than neat linear changes or isolated effects, the data revealed distributed, nonlinear, and frequency-specific dynamics that challenged traditional expectations. What emerged was a picture of neuroplastic recovery far more dynamic than previously reported, and perhaps one that redefined what "improvement" looks like in EEG-based regulation.

These findings build on early work by Cannon (2009), which utilized LORETA-based current density connectivity to identify self-regulatory cortical hubs. That study anticipated many of the now-standard ML and network approaches used in this field. In our current work, alpha and theta rhythms did not simply increase or decrease; rather, they reconfigured across individuals in heterogeneous yet functionally meaningful ways. These shifts reflected both successful and unsuccessful attempts at self-regulation, forming distributed networks rather than isolated regional effects. CSD changes were not random. They aligned with functional topographies of attention, inhibition, and mood regulation, particularly involving posterior hubs and left hemisphere integration.

To further examine the specificity of alpha-related changes, correlations between alpha-band CSD shifts and PAI symptom change were evaluated within the SUD group. As shown in Table 3, alpha-specific CSD changes demonstrated stronger and more consistent associations with reductions in aggression and depression than average power measures, particularly in precuneus and posterior cingulate regions, supporting a frequency- and location-specific mechanism of change.

Table 3
Alpha-Band Correlation with PAI Symptom Change (SUD Group)

ROI	PAI Target	*r* (Alpha Δ CSD)	*r* (Avg CSD Δ)
ROI2 (Lingual Gyrus)	Depression	−0.17	−0.00
ROI2	Aggression	**−0.45**	+0.02
ROI3 (Anterior cingulate)	Depression	−0.26	−0.10
ROI3	Aggression	−0.29	+0.23
ROI4 (Post. Cingulate)	Depression	+0.16	−0.09
ROI4	Aggression	−0.11	+0.24
ROI5 (Precuneus)	Aggression	−0.34	+0.11
ROI6 (Superior frontal gyrus)	Aggression	**−0.57**	**+0.27**

Note. Shows that alpha-specific CSD changes (especially in precuneus and posterior cingulate) track better with behavioral improvement (aggression, depression) than general power shifts. Negative correlations indicate symptom reduction is associated with increased alpha CSD. ROI 6 shows divergent patterns across alpha-specific vs. average power changes. This demonstrates increased coordination between alpha sub-bands, especially in precuneus, suggesting functional network integration posttraining.

The RCI allowed classification of participants into valid subgroups, each showing distinct neural response profiles. Both alpha synchronizers and desynchronizers exhibited meaningful clinical improvement, suggesting that adaptive self-regulation may proceed along different neural routes for different recipients of neurofeedback. This finding directly challenges the long-standing assumption that increased alpha is always the goal of training.

Differential response patterns across RCI-defined groups were further characterized by examining the most influential ROI–frequency–PAI relationships. As shown in Table 4, alpha and theta CSD changes in posterior cingulate, precuneus, anterior cingulate, and insular regions were consistently associated with somatic and anxiety-related subscales, supporting a network-level interpretation of responder classification.

ML analyses helped unpack complexity. SHAP values revealed nonlinear contributions across regions and frequencies, while PCA revealed structured learning profiles not visible through traditional statistics. These results strengthen the case for posterior alpha modulation as a core mechanism for rebalancing dysfunctional self-regulation, especially in individuals with high rates of trauma, psychiatric comorbidity, and motivational deficits (Cannon, 2025; Cannon et al., 2025). The effect size findings confirm regionally specific and frequency-sensitive plasticity in response to training, particularly within BA 19 components of the posterior self-regulation network. To further characterize frequency-specific changes within BA 19–related regions, effect sizes (Cohen's *d*) were computed across the full 1–40 Hz spectrum. As shown in Figure 12, distinct patterns of frequency-dependent modulation emerged, with the precuneus (ROI 6) demonstrating the strongest increases at higher frequencies, while the lingual gyrus (ROI 3) showed consistent suppression across low- to mid-frequency bands. Notably, while most effect sizes fell in the small-to-moderate range, they were accompanied by robust behavioral improvements, with group-level PAI deltas reaching a large effect size of $d = 0.85$ (Cannon et al., 2025). This dissociation illustrates a key point: even modest, frequency-specific neural changes can produce substantial clinical gains, particularly when training is anatomically constrained and behaviorally reinforced. These findings reinforce the precision of spectral targeting in LNFB and suggest that network-level reorganization, rather than bulk amplitude change, underlies clinically relevant improvement in individuals with SUD.

Rethinking SUD: From Trait to Developmental Trajectory

This study also contributes to a broader reframing of SUD, from fixed trait models to developmental, neuroplastic trajectories. Heritability estimates for addiction remain modest, and genome-wide studies have yet to identify stable predictors of risk (Kendler et al., 2003). More compelling evidence points to a convergence of early attachment disruption, social instability, trauma, and intrauterine substance exposure as key factors shaping the SUD phenotype. These factors often interact through the nervous system's regulatory architecture, not merely through learned behavior or moral failing.

Table 4
Summarizes the Mean and Standard Deviation of Delta Values for the 15 Most Significant Subscales Across Each RCI Group

Band	ROI (Region)	PAI Subscale	Mean SHAP
Alpha	ROI_4 (Posterior Cingulate)	somc_d	4.63
Alpha	ROI_6 (Superior Frontal Gyrus)	somc_d	3.9
Alpha	ROI_8 (Lingual Gyrus)	somc_d	2.93
Alpha	ROI_9 (Anterior Cingulate)	somd_d	2.65
Alpha	ROI_7 (Insula)	somd_d	2.5
Alpha	ROI_1 (Middle Frontal Gyrus)	somh_d	2.24
Alpha	ROI_4 (Posterior Cingulate)	somh_d	1.86
Alpha	ROI_9 (Anterior Cingulate)	somh_d	0.92
Alpha	ROI_4 (Posterior Cingulate)	anxc_d	2.77
Alpha	ROI_0 (Cuneus)	anxa_d	1.57
Alpha	ROI_5 (Precuneus)	anxa_d	2.21
Alpha	ROI_2 (Lingual Gyrus)	anxa_d	2.16
Theta	ROI_4 (Posterior Cingulate)	somc_d	4.86
Theta	ROI_7 (Insula)	somc_d	3.4
Theta	ROI_5 (Precuneus)	somc_d	3.15
Theta	ROI_6 (Superior Frontal Gyrus)	somd_d	4.74
Theta	ROI_1 (Middle Frontal Gyrus)	somd_d	1.6
Theta	ROI_8 (Lingual Gyrus)	somd_d	1.24
Theta	ROI_5 (Precuneus)	somh_d	4.56
Theta	ROI_1 (Middle Frontal Gyrus)	somh_d	1.82
Theta	ROI_2 (Lingual Gyrus)	somh_d	1.15
Theta	ROI_9 (Anterior Cingulate)	anxc_d	4.01
Theta	ROI_5 (Precuneus)	anxc_d	2.4
Theta	ROI_3 (Anterior Cingulate)	anxc_d	2.08
Theta	ROI_8 (Lingual Gyrus)	anxa_d	2.24
Theta	ROI_2 Lingual Gyrus)	anxa_d	2.05

Note. The differential response patterns align with the underlying neurophysiological distinctions derived from CSD shifts, providing convergent validity for the RCI-based responder classification.

Many substance abuse clients are diagnosed shortly after detoxification, yet their brains often struggle to restructure social, emotional, and physiological stability, even after 2 weeks to 5 months of abstinence (Nixon & Lewis, 2020). Moreover, SUD histories frequently overlap with prenatal exposures, when parents-to-be conceive while under the influence of substances or ‘safe’ psychiatric medications. For example, prenatal selective serotonin reuptake inhibitors (SSRI) exposure may lead to subtle but persistent disruptions in neurodevelopment, especially in domains of attention, emotion regulation, and executive function (Koc et al., 2023). Thus, SUD and PDE may be better understood as sequential dysregulation spanning generations. Critically, many individuals with SUD histories go on to conceive children under the influence of alcohol, nicotine, cannabis, opioids, or prescribed psychiatric medications. Even when deemed “safe,” such exposures, particularly to SSRIs, may contribute to subtle but durable neurodevelopmental disruptions in the child, particularly in domains related to attention, emotion regulation, and executive control (Croen et al., 2011; Gentile, 2010; Oberlander et al., 2007). As such, SUD and PDE may be viewed not as separate conditions, but as sequential iterations of dysregulation, echoing across generations. This

reframing implies that interventions aimed at restoring rhythms and self-regulation in SUD patients may have cascading effects beyond the individual. By improving brain network integrity and adaptive function, neurofeedback may serve as both a therapeutic and preventative tool.

Implications for Clinical Neurofeedback

The current findings support the use of individualized, voxel-level neurofeedback protocols guided by ML. Both responders and nonresponders showed meaningful information patterns in their CSD changes, with responders exhibiting both increases and decreases in alpha power, depending on baseline state. Importantly, desynchronization should not be seen as a failure, but as a viable pathway to regulation. This challenges a foundational bias in the neurofeedback field, that amplitude increases are inherently good (Bell et al., 2019; Riha, 2021).

Consistent with prior work on lateralized function, left frontal and left posterior ROI emerged as major contributors to regulation and behavioral improvement. ROI 2 (posterior parietal cortex) and ROI 3 (anterior cingulate cortex) were repeatedly flagged in SHAP analyses, and are known to support attentional reorientation, emotional regulation, and inhibition, core deficits in many SUD populations. SUD individuals in recovery tend to struggle with social, emotional and adaptive skills development, and often experience the self and world in unfavorable ways (Cannon et al., 2008). A further consideration is the perceived “threat” of neurofeedback to traditional mental health practice. It is critical to emphasize that EEG or neuroimaging techniques are not at a stage where data can simply be programmed into the brain. Neurofeedback does not implant skills, values, or social knowledge; rather, it facilitates the brain’s intrinsic capacity for self-regulation by promoting adaptive oscillatory states and functional connectivity. Translating these neurophysiological gains into meaningful life changes still requires social learning, cognitive restructuring, and therapeutic engagement. In other words, neurofeedback primes the neural architecture for regulation, but clients must still be taught how to apply these capacities in real-world contexts—social, emotional, and adaptive—through structured, purposeful, and insight-oriented interventions. Thus, neurofeedback should not be regarded as a replacement for psychotherapy or education but as a complementary method that enhances their efficacy by stabilizing the neural foundations upon which skills are built (Hammond, 2011; Micoulaud-Franchi & Fovet, 2016).

More broadly, the findings align with literature implicating left-hemisphere hypoactivity in mood and affective disorders (Davidson, 2004). In particular, left posterior structures such as the precuneus and temporoparietal junction (TPJ) appear essential to internal narrative, self-related thought, and receptive language. Disruption in these areas may impair the scaffolding of identity and hinder access to autobiographical memory, a pattern commonly observed in addiction, trauma, and depression (Gibson et al., 2022; Zhang et al, 2025).

The spectral distribution of training-related cortical change revealed frequency- and region-specific modulation across BA 19 ROI. Alpha-band frequencies (8–13 Hz) showed the strongest training effects in ROI 2 (lingual gyrus), ROI 3 (precuneus), and ROI 5 (anterior cingulate), with moderate effect sizes (Cohen’s d = 0.29–0.33). ROI 6 (superior frontal gyrus) showed selective low beta modulation (~30–34 Hz), indicating dynamic plasticity across multiple bands. Importantly, these modest physiological effects were accompanied by a significant group-level PAI improvement (d = 0.85), highlighting the power of frequency-specific modulation to induce meaningful behavioral shifts across heterogenous populations (Cannon et al., 2025).

The posterior-to-frontal shift observed in regression-weighted networks and PCA loading vectors suggests that regulation is not about isolated activation, but dynamic redistribution. Effective self-regulation appears to require a realignment of attentional control and default mode systems, a process that may be visible only through network-level, multivariate models like those used here.

One of the clearest outcomes of this study is the confirmation that frequency-specific modulation, interregional coordination, and network-level reorganization do occur because of neurofeedback, particularly when guided by LORETA-based CSD training. While many traditional neurofeedback models have reported localized amplitude changes, the present findings provide direct evidence that training can induce structured, nonlinear alterations in frequency distribution (e.g., alpha desynchronization or redistribution), comodulation across cortical hubs, and emergent connectivity patterns indicative of restored regulatory function.

These outcomes were not inferred from surface amplitudes or visual inspection but derived from anatomically constrained, voxel-wise data

interpreted using multivariate ML models. Such models, especially when paired with SHAP analysis and PCA, identified nonlinear and distributed changes that would be invisible to univariate statistics or visual EEG review. The emergent pattern of posterior-to-frontal redistribution, frequency-specific ROI involvement, and group-stratified regulatory profiles represents a compelling case for network-based, frequency-sensitive neurofeedback analytics.

The network visualization in Figure 7 highlights a rare but critically important phenomenon: not only do cortical regions demonstrate posttraining changes in alpha and theta oscillatory dynamics, but these neural shifts are meaningfully linked to validated subscales of psychological symptoms and experiential processes. The presence of both alpha-only (green) and theta-only (orange) connections underscores frequency-specific contributions to regulation, while the purple "shared" links reveal overlapping spectral signatures of symptom-related variance. Such associations extend beyond simple electrophysiological modulation, suggesting that certain ROI–PAI relationships may constitute neural "flags" of disorder phenotypes, marking enduring vulnerabilities in attention, affect regulation, and self-related processing. This bridging of EEG source dynamics with psychometric measures is seldom achieved in neurofeedback research, where electrophysiological changes are often reported without concurrent demonstration of clinical or personality correlates. Importantly, the appearance of left posterior (precuneus, parietal) and left middle frontal and anterior cingulate regions within these networks is consistent with prior work identifying these loci as hubs of self-regulation and inhibitory control, both of which are disrupted in substance use and related disorders (Enriquez-Geppert et al., 2017). Moreover, the convergence of ROI-based alpha and theta connectivity with subscales reflecting mood, somatization, paranoia, and substance-related experiences parallels broader evidence that cross-frequency coupling within default mode and executive networks underpins vulnerability across psychiatric dimensions (Huster et al., 2013; Menon, 2011). Thus, the present findings suggest that individualized neurofeedback training does not merely shift oscillatory power in isolation but also reshapes functional couplings that map onto clinically relevant psychological dimensions, supporting the promise of voxel-level, ML-guided approaches for uncovering network-level biomarkers of both disorder and recovery.

Together, these observations lay the groundwork for a new generation of interventions: systems that adapt to individual learning rhythms, map actual neural engagement, and evolve through feedback-informed AI rather than static protocols. Current effect sizes and lack of truly standardized procedures beg for a system that can do what humans to date have failed to accomplish, understand and then treat substance abuse problems. In order for AI and ML to function meaningfully in brain research, regardless of the method employed, standardized procedures and protocols are essential. Without consistency in data acquisition, preprocessing, and labeling, even the most advanced models will amplify noise rather than extract signal. The application of ML and AI to EEG and other physiological modalities holds enormous promise but only if those methods are grounded in structured, standardized acquisition and analysis procedures. Unlike exploratory hypothesis testing, which may tolerate variability, ML depends on coherent, repeatable input. Without clearly defined protocols for data collection, preprocessing, feature selection, and target labeling, even the most powerful algorithms will simply mirror noise. In the neurofeedback literature, as well as in fMRI, qEEG, and other imaging domains, inconsistent methods have led to conflicting outcomes and questionable reproducibility. For AI to function as a generative tool in neuroscience, capable of detecting patterns, predicting response, and refining treatment, its foundation must be stability. That means using physiologically valid models, reliable data pipelines, and rigorous documentation at every step. The brain is already a noisy and dynamic system; when experimental variability is added on top of that, the result is analytical confusion rather than insight. Structure enables signal to emerge, and in the absence of that structure, AI will only mirror our uncertainty.

Future research is needed to apply similar modeling and analytic frameworks to more traditional surface-based neurofeedback approaches, including SMR, theta/beta, and *Z*-score protocols. Without comparable data and structure, direct comparisons remain difficult. However, the present findings suggest that current source-guided neurofeedback may offer a more reliable and physiologically grounded means of accessing and modulating core self-regulatory networks with particular focus in clinical populations with complex, distributed dysregulation such as those with SUD.

Limitations and Future Directions

This study has several limitations. The sample, while well-characterized, was drawn entirely from incarcerated adults, limiting generalizability to community-based or adolescent SUD populations. While CSD offers improved spatial resolution over surface EEG, it still lacks the precision of fMRI or magnetoencephalography (MEG) source analysis. Future work should include longitudinal studies, additional neuroimaging modalities, and developmental extensions to better understand intergenerational effects of rhythm-based dysregulation.

Moreover, although our ML models offered interpretable and accurate classifications, they are ultimately constrained by the quality of input data. As any practitioner outside of tightly controlled laboratory settings recognizes, artifact-free EEG baselines are virtually unattainable in real-world clinical and forensic settings. This challenge is amplified when contrasting surface EEG with CSD approaches. While surface recordings are more vulnerable to volume conduction, reference contamination, and peripheral artifacts, CSD estimation attenuates many of these issues by enhancing spatial resolution and isolating cortical generators. Nonetheless, even CSD methods depend on the integrity of the raw recordings, requiring careful artifact management, standardized protocols for baselines, training and preprocessing pipelines, and clear target definitions. The generalizability of our findings therefore hinges on methodological alignment across laboratories and practitioners. Without such convergence, neurofeedback will remain heterogeneous, and the translational promise of AI-driven insights will be limited (Kayser & Tenke, 2015; Ros et al., 2020).

Despite over 6 decades of progress in neuroscience and diagnostic psychiatry, the field has yet to isolate a single, biologically valid “disorder” in the brain. This does not necessarily imply that mental disorders are fictitious but rather that our current definitions and diagnostic frameworks may be misaligned with the biological realities they intend to capture. The greatest challenge and perhaps the greatest promise of AI and ML lies in their potential to clarify and deconstruct this diagnostic ambiguity. At present, psychiatric classifications remain largely syndromal, relying on subjective criteria rather than objective neural signatures (Insel et al., 2010). Disorders such as depression, ADHD, or schizophrenia have shown high internal heterogeneity and poor predictive utility, even when examined through decades of neuroimaging and genetics research (Elliott et al., 2018; Kapur et al., 2012). Advanced ML tools provide an opportunity to move beyond symptom clusters and instead characterize disorders by measurable, network-based features that evolve over time and context.

For example, work by Drysdale et al. (2017) used resting-state fMRI and ML to identify four distinct neurophysiological subtypes of depression, each with unique connectivity patterns and treatment responses. Similarly, Dwyer et al. (2018) demonstrated that ML approaches can outperform traditional methods in identifying functional brain patterns in schizophrenia, patterns that cross diagnostic boundaries and reveal unexpected dimensions of psychopathology. These studies highlight the urgent need to rethink disorder classifications, not as fixed categories, but as dynamic profiles embedded in the structure of brain networks. Until such models are widely adopted, misclassification and treatment mismatch will remain significant barriers to progress. We have much work to do in this regard, but the tools now exist to do it.

Conclusion

In this study, we did not aim to prove a theory, but to interrogate a reality: What changes, and how, when a brain with SUD undergoes neurofeedback at a known self-regulatory hub? Using ML tools to decode EEG-derived current density and behavior, we found robust and interpretable patterns of network reorganization, tied to individual learning profiles and behavioral outcomes. These findings support a shift in how we view addiction, not as a moral failure or fixed trait, but as a dynamic, frequency-sensitive disruption in regulatory function.

This reframing, grounded in real-world data and validated by nonlinear models, sets the stage for a more precise and humane understanding of SUD. AI will not solve addiction, but it may finally allow us to ask the right questions and listen to what the brain is trying to say.

The present work represents a first step in decoding self-regulation in SUD using CSD-informed neurofeedback and ML. Moving forward, we will extend this framework to children with in utero drug exposure (IUDE), as well as normative and heterogeneous adolescent and adult samples, to clarify developmental trajectories of rhythmic self-regulation and identify potential early biomarkers of risk. Parallel to this research agenda, we have developed stand-alone software capable of delivering the current LNFB protocol, along with

additional source-based protocols, across a range of EEG devices. This platform is designed for flexible implementation in diverse clinical and research settings. Beyond local delivery, we are building cloud-based infrastructure for automated artifact detection, ROI extraction, and large-scale data integration. These advances will allow for scalable, reproducible, and standardized neurofeedback across populations, creating the possibility of real-time precision interventions that bridge neuroscience, clinical practice, and AI-driven analytics.

Importantly, the future of this work must also emphasize equity and access. Neurofeedback informed by ML and source-space modeling should not remain limited to specialized or privileged contexts. Our goal is to ensure that these tools are available to all in-need populations, including children, incarcerated individuals, and communities historically underserved by mental health systems, and to the professionals who work alongside them. By building accessible, strict, evidence-based platforms, we aim to extend the benefits of rhythmic self-regulation beyond the laboratory and into the settings where they are needed most.

Author Declarations

The author thanks the developers and maintainers of open-source scientific software libraries that made this work possible, including NumPy, pandas, SciPy, scikit-learn, UMAP-learn, and Matplotlib. Portions of the data processing, analysis, and manuscript drafting were supported by the use of large language models as a writing and code-assistance tool. All analytic decisions, interpretations, and conclusions are solely the responsibility of the author. A provisional patent application has been filed related to the methods and systems described in this study, including the LNFB training architecture and ML model for CSD classification.

References

Baldwin, D. R., Cannon, R., Fischer, S., & Kivisto, K. (2011). The inverse of psychopathology: A Loreta EEG and cortisol examination. *Journal of Neurotherapy, 15*(4), 374–388. https://doi.org/10.1080/10874208.2011.623095

Barry, R. J., Clarke, A. R., Johnstone, S. J., Magee, C. A., & Rushby, J. A. (2007). EEG differences between eyes-closed and eyes-open resting conditions. *Clinical Neurophysiology, 118*(12), 2765–2773. https://doi.org/10.1016/j.clinph.2007.07.028

Başar, E., Başar-Eroglu, C., Karakaş, S., & Schürmann, M. (2001). Gamma, alpha, delta, and theta oscillations govern cognitive processes. *International Journal of Psychophysiology, 39*(2–3), 241–248. https://doi.org/10.1016/s0167-8760(00)00145-8

Bassett, D. S., & Sporns, O. (2017). Network neuroscience. *Nature Neuroscience, 20*(3), 353–364. https://doi.org/10.1038/nn.4502

Bazanova, O. M., & Vernon, D. (2014). Interpreting EEG alpha activity. *Neuroscience & Biobehavioral Reviews, 44*, 94–110. https://doi.org/10.1016/j.neubiorev.2013.05.007

Belenko, S., & Peugh, J. (2005). Estimating drug treatment needs among state prison inmates. *Drug and Alcohol Dependence, 77*(3), 269–281. https://doi.org/10.1016/j.drugalcdep.2004.08.023

Bell, A. N., Moss, D., & Kallmeyer, R. J. (2019). Healing the neurophysiological roots of trauma: A controlled study examining LORETA *z*-score neurofeedback and HRV biofeedback for chronic PTSD. *NeuroRegulation, 6*(2), 54–70. https://doi.org/10.15540/nr.6.2.54

Breiman, L. (2001). Random forests. *Machine Learning, 45*(1), 5–32. https://doi.org/10.1023/A:1010933404324

Brewer, J. A., Garrison, K. A., & Whitfield-Gabrieli, S. (2013). What about the "self" is processed in the posterior cingulate cortex? *Frontiers in Human Neuroscience, 7*, Article 647. https://doi.org/10.3389/fnhum.2013.00647

Buckner, R. L., Andrews-Hanna, J. R., & Schacter, D. L. (2008). The brain's default network. *Annals of the New York Academy of Sciences, 1124*(1), 1–38. https://doi.org/10.1196/annals.1440.011

Cannon, R. L. (2009). *Functional connectivity of EEG LORETA in cortical core components of the self and the default network (DNt) of the brain*. [PhD dissertation, University of Tennessee]. https://trace.tennessee.edu/utk_graddiss/571

Cannon, R. L. (2014). Parietal foci for attention-deficit/hyperactivity disorder: Targets for LORETA neurofeedback with outcomes. *Biofeedback, 42*(2), 47–57. https://doi.org/10.5298/1081-5937-42.2.01

Cannon, R. L. (2025). Quantifying self-regulation: Neuroevolutionary insights from precuneus alpha modulation via LORETA neurofeedback. *NeuroRegulation, 12*(2), 65–81. https://doi.org/10.15540/nr.12.2.65

Cannon, R. L., Baldwin, D. R., Diloreto, D. J., Phillips, S. T., Shaw, T. L., & Levy, J. J. (2014). LORETA neurofeedback in the precuneus: Operant conditioning in basic mechanisms of self-regulation. *Clinical EEG and Neuroscience, 45*(4), 238–248. https://doi.org/10.1177/1550059413512796

Cannon, R. L., Baldwin, D. R., Shaw, T. L., Diloreto, D. J., Phillips, S. M., Scruggs, A. M., & Riechel, B. D. (2012). Reliability of quantitative EEG (qEEG) measures and LORETA current source density at 30 days. *Neuroscience Letters, 518*(1), 27–31. https://doi.org/10.1016/j.neulet.2012.04.035

Cannon, R., Lubar, J., & Baldwin, D. (2008). Self-perception and experiential schemata in the addicted brain. *Applied and Psychophysiology Biofeedback, 33*(4), 223–238. https://doi.org/10.1007/s10484-008-9067-9

Cannon, R., Lubar, J., Thornton, K., Wilson, S., & Congedo, M. (2004). Limbic beta activation and LORETA: Can hippocampal and related limbic activity be recorded and changes visualized using LORETA in an affective memory condition? *Journal of Neurotherapy, 8*(4), 5–24. https://doi.org/10.1300/J184v08n04_02

Cannon, R. L., Mills, C., Geroux, M., Zhart, L. A., Boluyt, K., Webber, R., & Cook, D. (2025). LORETA neurofeedback at precuneus: A standard approach for use in incarcerated populations with substance use problems. *NeuroRegulation, 12*(3), 213–233. https://doi.org/10.15540/nr.12.3.213

Cavanagh, J. F., & Frank, M. J. (2014). Frontal theta as a mechanism for cognitive control. *Trends in Cognitive Sciences, 18*(8), 414–421. https://doi.org/10.1016/j.tics.2014.04.012

Cavanna, A. E., & Trimble, M. R. (2006). The precuneus: A review of its functional anatomy and behavioural correlates. *Brain, 129*(3), 564–583. https://doi.org/10.1093/brain/awl004

Coan, J. A., & Allen, J. J. B. (2004). Frontal EEG asymmetry as a moderator and mediator of emotion. *Biological Psychology, 67*(1–2), 7–50. https://doi.org/10.1016/j.biopsycho.2004.03.002

Croen, L. A., Grether, J. K., Yoshida, C. K., Odouli, R., & Hendrick, V. (2011). Antidepressant use during pregnancy and childhood autism spectrum disorders. *Archives of General Psychiatry, 68*(11), 1104–1112. https://doi.org/10.1001/archgenpsychiatry.2011.73

Davidson, R. J. (2004). What does the prefrontal cortex "do" in affect: Perspectives on frontal EEG asymmetry research. *Biological Psychology, 67*(1–2), 219–233. https://doi.org/10.1016/j.biopsycho.2004.03.008

Drysdale, A. T., Grosenick, L., Downar, J., Dunlop, K., Mansouri, F., Meng, Y., Fetcho, R. N., Zebley, B., Oathes, D. J., Etkin, A., Schatzberg, A. F., Sudheimer, K., Keller, J., Mayberg, H. S., Gunning, F. M., Alexopoulos, G. S., Fox, M. D., Pascual-Leone, A., Voss, H. U. ... & Liston, C. (2017). Resting-state connectivity biomarkers define neurophysiological subtypes of depression. *Nature Medicine, 23*(1), 28–38. https://doi.org/10.1038/nm.4246

Dwyer, D. B., Falkai, P., & Koutsouleris, N. (2018). Machine learning approaches for clinical psychology and psychiatry. *Annual Review of Clinical Psychology, 14*, 91–118. https://doi.org/10.1146/annurev-clinpsy-032816-045037

Enriquez-Geppert, S., Huster, R. J., & Herrmann, C. S. (2017). EEG-neurofeedback as a tool to modulate cognition and behavior: A review tutorial. *Frontiers in Human Neuroscience, 11*, Article 51. https://doi.org/10.3389/fnhum.2017.00051

Elliott, M. L., Romer, A., Knodt, A. R., & Hariri, A. R. (2018). A connectome-wide functional signature of transdiagnostic risk for mental illness. *Biological Psychiatry, 84*(6), 452–459. https://doi.org/10.1016/j.biopsych.2018.03.012

Friston, K. (2010). The free-energy principle: A unified brain theory? *Nature Reviews Neuroscience, 11*(2), 127–138. https://doi.org/10.1038/nrn2787

Gentile, S. (2010). Neurodevelopmental effects of prenatal exposure to psychotropic medications. *Depression and Anxiety, 27*(7), 675–686. https://doi.org/10.1002/da.20706

Gibson, B. C., Vakhtin, A., Clark, V. P., Abbott, C. C., & Quinn, D. K. (2022). Revisiting hemispheric asymmetry in mood regulation: Implications for rTMS for major depressive disorder. *Brain Sciences, 12*(1), Article 112. https://doi.org/10.3390/brainsci12010112

Gigerenzer, G. (2004). Mindless statistics. *The Journal of Socio-Economics, 33*(5), 587–606. https://doi.org/10.1016/j.socec.2004.09.033

Grace, A. A. (1991). Phasic versus tonic dopamine release and the modulation of dopamine system responsivity: A hypothesis for the etiology of schizophrenia. *Neuroscience, 41*(1), 1–24. https://doi.org/10.1016/0306-4522(91)90196-U

Gusnard, D. A., & Raichle, M. E. (2001). Searching for a baseline: Functional imaging and the resting human brain. *Nature Reviews Neuroscience, 2*(10), 685–694. https://doi.org/10.1038/35094500

Hammond, D. C. (2011). What is neurofeedback: An update. *Journal of Neurotherapy, 15*(4), 305–336. https://doi.org/10.1080/10874208.2011.623090

Haugg, A., Sladky, R., Skouras, S., McDonald, A., Craddock, C., Kirschner, M., Herdener, M., Koush, Y., Papoutsi, M., Keynan, J. N., Hendler, T., Cohen Kadosh, K., Zich, C., MacInnes, J., Adcock, R. A., Dickerson, K., Chen, N. K., Young, K., Bodurka, J., Yao, S., … Scharnowski, F. (2020). Can we predict real-time fMRI neurofeedback learning success from pretraining brain activity? *Human Brain Mapping, 41*(14), 3839–3854. https://doi.org/10.1002/hbm.25089

Huster, R. J., Enriquez-Geppert, S., Lavallee, C. F., Falkenstein, M., & Herrmann, C. S. (2013). Electroencephalography of response inhibition tasks: Functional networks and cognitive contributions. *International Journal of Psychophysiology, 87*(3), 217–233. https://doi.org/10.1016/j.ijpsycho.2012.08.001

Insel, T. R., Cuthbert, B. N., Garvey, M., Heinssen, R., Pine, D. S., Quinn, K., Sanislow, C., & Wang, P. (2010). Research domain criteria (RDoC): Toward a new classification framework for research on mental disorders. *American Journal of Psychiatry, 167*(7), 748–751. https://doi.org/10.1176/appi.ajp.2010.09091379

Ioannidis, J. P. A. (2018). The challenge of reforming nutritional epidemiologic research. *JAMA, 320*(10), 969–970. https://doi.org/10.1001/jama.2018.11025

Jacobson, N. S., & Truax, P. (1991). Clinical significance: A statistical approach to defining meaningful change in psychotherapy research. *Journal of Consulting and Clinical Psychology, 59*(1), 12–19. https://doi.org/10.1037/0022-006X.59.1.12

Jensen, O., & Mazaheri, A. (2010). Shaping functional architecture by oscillatory alpha activity: Gating by inhibition. *Frontiers in Human Neuroscience*, *4*, Article 186. https://doi.org/10.3389/fnhum.2010.00186

Kapur, S., Phillips, A. G., & Insel, T. R. (2012). Why has it taken so long for biological psychiatry to develop clinical tests and what to do about it? *Molecular Psychiatry, 17*(12), 1174–1179. https://doi.org/10.1038/mp.2012.105

Kayser, J., & Tenke, C. E. (2015). Issues and considerations for using the scalp surface Laplacian in EEG/ERP research: A tutorial review. *International Journal of Psychophysiology, 97*(3), 189–209. https://doi.org/10.1016/j.ijpsycho.2015.04.012

Kelley, L., Strunk, W., Cannon, R., & Leighton, J. (2019). EEG source localization and attention differences between children exposed to drugs in utero and those with attention-deficit/hyperactivity disorder: A pilot study. *NeuroRegulation, 6*(1), 23–37. https://doi.org/10.15540/nr.6.1.23

Kendler, K. S., Jacobson, K. C., Prescott, C. A., & Neale, M. C. (2003). Specificity of genetic and environmental risk factors for use and abuse/dependence of cannabis, cocaine, hallucinogens, sedatives, stimulants, and opiates. *American Journal of Psychiatry, 160*(4), 687–695. https://doi.org/10.1176/appi.ajp.160.4.687

Koc, D., Tiemeier, H., Stricker, B. H., Muetzel, R. L., Hillegers, M., & El Marroun, H. (2023). Prenatal antidepressant exposure and offspring brain morphologic trajectory. *JAMA Psychiatry, 80*(12), 1208–1217. https://doi.org/10.1001/jamapsychiatry.2023.3161

Koponen, A. M., Nissinen, N.-M., Gissler, M., Autti-Rämö, I., Sarkola, T., & Kahila, H. (2020). Prenatal substance exposure, adverse childhood experiences and diagnosed mental and behavioral disorders – A longitudinal register-based matched cohort study in Finland. *SSM - Population Health, 11*, Article 100625. https://doi.org/10.1016/j.ssmph.2020.100625

Klimesch, W. (1999). EEG alpha and theta oscillations reflect cognitive and memory performance: A review and analysis. *Brain Research Reviews, 29*(2–3), 169–195. https://doi.org/10.1016/S0165-0173(98)00056-3

Knyazev, G. G. (2013). EEG correlates of self-referential processing. *Frontiers in Human Neuroscience, 7*, Article 264. https://doi.org/10.3389/fnhum.2013.00264

Leech, R., & Sharp, D. J. (2014). The role of the posterior cingulate cortex in cognition and disease. *Brain, 137*(1), 12–32. https://doi.org/10.1093/brain/awt162

Lundberg, S. M., & Lee, S.-I. (2017). A unified approach to interpreting model predictions. In *Advances in neural information processing systems* (Vol. 30). https://doi.org/10.48550/arXiv.1705.07874

Menon, V. (2011). Large-scale brain networks and psychopathology: A unifying triple network model. *Trends in*

Cognitive Sciences, 15(10), 483–506. https://doi.org/10.1016/j.tics.2011.08.003

Mericle, A. A., Casaletto, K., Knoblach, D., Brooks, A. C., & Carise, D. (2010). Drug policy by popular sovereignty. *Journal of Drug Issues, 40*(4), 819–839. https://doi.org/10.1177/002204261004000404

Micoulaud-Franchi, J. A., & Fovet, T. (2016). Neurofeedback: Time needed for a promising non-pharmacological therapeutic method. *The Lancet Psychiatry, 3*(9), Article e16. https://doi.org/10.1016/S2215-0366(16)30189-4

Mitchell, D. J., McNaughton, N., Flanagan, D., & Kirk, I. J. (2008). Frontal-midline theta from the perspective of hippocampal "theta." *Progress in Neurobiology, 86*(3), 156–185. https://doi.org/10.1016/j.pneurobio.2008.09.005

Morey, L. C. (1991). *Personality Assessment Inventory: Professional manual*. Psychological Assessment Resources.

Mumola, C. J., & Karberg, J. C. (2006). *Drug use and dependence, state and federal prisoners, 2004* (NCJ 213530). U.S. Department of Justice, Bureau of Justice Statistics.

Nixon, S. J., & Lewis, B. (2020). Brain structure and function in recovery. *Alcohol Research: Current Reviews, 40*(3), Article 04. https://doi.org/10.35946/arcr.v40.3.04

Northoff, G., Heinzel, A., de Greck, M., Bermpohl, F., Dobrowolny, H., & Panksepp, J. (2006). Self-referential processing in our brain—A meta-analysis of imaging studies on the self. *NeuroImage, 31*(1), 440–457. https://doi.org/10.1016/j.neuroimage.2005.12.002

Oberlander, T. F., Reebye, P., Misri, S., Papsdorf, M., Kim, J., & Grunau, R. E. (2007). Externalizing and attentional behaviors in children of depressed mothers treated with a selective serotonin reuptake inhibitor antidepressant during pregnancy. *Archives of Pediatrics & Adolescent Medicine, 161*(1), 22–29. https://doi.org/10.1001/archpedi.161.1.22

Open Science Collaboration. (2015). Estimating the reproducibility of psychological science. *Science, 349*(6251), Article aac4716. https://doi.org/10.1126/science.aac4716

Pascual-Marqui, R. D., Michel, C. M., & Lehmann, D. (1994). Low resolution electromagnetic tomography: A new method for localizing electrical activity in the brain. *International Journal of Psychophysiology, 18*(1), 49–65. https://doi.org/10.1016/0167-8760(84)90014-x

Pascual-Marqui, R. D. (2002). Standardized low-resolution brain electromagnetic tomography (sLORETA): Technical details. *Methods and Findings in Experimental and Clinical Pharmacology, 24*(Suppl D), 5–12.

Pascual-Marqui, R. D., Esslen, M., Kochi, K., & Lehmann, D. (2002). Functional imaging with low-resolution brain electromagnetic tomography (LORETA): A review. *Methods and Findings in Experimental and Clinical Pharmacology, 24* (Suppl C), 91–95.

Peniston, E. G., & Kulkosky, P. J. (1989). Alpha–theta brainwave training and beta-endorphin levels in alcoholics. *Alcoholism: Clinical and Experimental Research, 13*(2), 271–279. https://doi.org/10.1111/j.1530-0277.1989.tb00325.x

Riha, C. (2021). *Developing individual neurofeedback: Latent class modeling of responder trajectories in alpha-band training* [Doctoral dissertation]. University of Zurich.

Ros, T., Enriquez-Geppert, S., Zotev, V., Young, K. D., Wood, G., Whitfield-Gabrieli, S., Wan, F., Vuilleumier, P., Vialatte, F., Van De Ville, D., Todder, D., Surmeli, T., Sulzer, J. S., Strehl, U., Sterman, M. B., Steiner, N. J., Sorger, B., Soekadar, S. R., Sitaram, R., … Thibault, R. T. (2020). Consensus on the reporting and experimental design of clinical and cognitive-behavioural neurofeedback studies (CRED-nf checklist). *Brain, 143*(6), 1674–1685. https://doi.org/10.1093/brain/awaa009

Scheeringa, R., Petersson, K. M., Oostenveld, R., Norris, D. G., Hagoort, P., & Bastiaansen, M. C. M. (2008). Trial-by-trial coupling between EEG and BOLD identifies networks related to alpha and theta EEG power increases during working memory maintenance. *NeuroImage, 44*(3), 1224–1238. https://doi.org/10.1016/j.neuroimage.2008.08.041

Sitaram, R., Ros, T., Stoeckel, L., Haller, S., Scharnowski, F., Lewis-Peacock, J., Weiskopf, N., Blefari, M. L., Rana, M., Oblak, E., Birbaumer, N., & Sulzer, J. (2017). Closed-loop brain training: The science of neurofeedback. *Nature Reviews Neuroscience, 18*(2), 86–100. https://doi.org/10.1038/nrn.2016.164

Zhang, L., Qin, K., Pan, N., Xu, H., & Gong, Q. (2025). Shared and distinct patterns of default mode network in major depressive disorder and bipolar disorder: A comparative meta-analysis. *Journal of Affective Disorders, 368*, 23–32. https://doi.org/10.1016/j.jad.2024.09.021

Zhou, Y., Dougherty, J. H. Jr., Hubner, K. F., Bai, B., Cannon, R. L., & Hutson, R. K. (2008). Abnormal connectivity in the posterior cingulate and hippocampus in early Alzheimer's disease and mild cognitive impairment. *Alzheimer's & Dementia, 4*(4), 265–270. https://doi.org/10.1016/j.jalz.2008.04.006

Received: August 26, 2025
Accepted: October 1, 2025
Published: March 31, 2026